

TOPICAL REVIEW • OPEN ACCESS

Biomedical application of optical fibre sensors

To cite this article: R Correia *et al* 2018 *J. Opt.* **20** 073003

View the [article online](#) for updates and enhancements.

Related content

- [Roadmap on optical sensors](#)
Mário F S Ferreira, Enrique Castro-Camus, David J Ottaway *et al.*
- [Response of the transmission spectrum of tapered optical fibres to the deposition of a nanostructured coating](#)
R Jarzebinska, C S Cheung, S W James *et al.*
- [Biomedical sensors using optical fibres](#)
Anna Grazia Mignani and Francesco Baldini



IOP | ebooks™

Bringing you innovative digital publishing with leading voices to create your essential collection of books in STEM research.

Start exploring the collection - download the first chapter of every title for free.

Topical Review

Biomedical application of optical fibre sensors

R Correia¹, S James² , S-W Lee³ , S P Morgan¹  and S Korposh^{1,4} ¹ Optics and Photonics Group, Faculty of Engineering, University of Nottingham, Nottingham, NG7 2RD, United Kingdom² Engineering Photonics, Cranfield University, Cranfield, Bedford MK43 0AL, United Kingdom³ Graduate School of Environmental Engineering, University of Kitakyushu, Kitakyushu, 808-0135, JapanE-mail: s.korposh@nottingham.ac.uk

Received 22 May 2017, revised 8 May 2018

Accepted for publication 21 May 2018

Published 8 June 2018



CrossMark

Abstract

Optical fibre sensors (OFS), as a result of their unique properties such as small size, no interference with electromagnetic radiation, high sensitivity and the ability to design multiplexed or distributed sensing systems, have found applications ranging from structural health monitoring to biomedical and point of care instrumentation. While the former represents the main commercial application for OFS, there is body of literature concerning the deployment of this versatile sensing platform in healthcare. This paper reviews the different types of OFS and their most recent applications in healthcare. It aims to help clinicians to better understand OFS technology and also provides an overview of the challenges involved in the deployment of developed technology in healthcare. Examples of the application of OFS in healthcare are discussed with particular emphasis on recently (2015–2017) published works to avoid replicating recent review papers. The majority of the work on the development of biomedical OFS stops at the laboratory stage and, with a few exceptions, is not explored in healthcare settings. OFSs have yet to fulfil their great potential in healthcare and methods of increasing the adoption of medical devices based on optical fibres are discussed. It is important to consider these factors early in the device development process for successful translation of the developed sensors to healthcare practice.

Keywords: optical fibre sensors, biomedical, healthcare

(Some figures may appear in colour only in the online journal)

1. Introduction

This paper reviews recent achievements in the area of optical fibre sensors (OFS) and the application of the technology in healthcare. The first section of the paper introduces the principle of operation of optical fibres as a sensing platform, discussing

different types and configurations of OFS and difficulties of comparison between them with an aim of providing an overview of OFS capabilities for end users (clinicians/healthcare workers). The sensors are then classified according to the measurands used in healthcare and are classified as physical (temperature, strain, pressure) and biochemical (volatile organic compounds (VOCs), biomarkers, proteins, immuno-sensors). Examples of the application of OFS in healthcare are discussed with particular emphasis on recently (2015–2017) published works to avoid replicating recent review papers on pressure [1], temperature [2] and biosensor [3] applications in healthcare. The use of optical fibres to deliver and collect light in applications such as laser Doppler flowmetry and oximetry are mentioned only briefly, as

⁴ Author to whom any correspondence should be addressed.



Original content from this work may be used under the terms of the [Creative Commons Attribution 3.0 licence](https://creativecommons.org/licenses/by/3.0/). Any further distribution of this work must maintain attribution to the author(s) and the title of the work, journal citation and DOI.

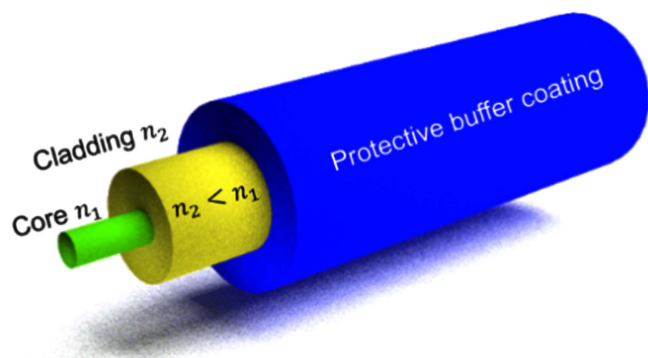


Figure 1. Schematic illustration of standard single mode telecoms silica optical fibre consisting of the core (diameter 4–10 μm), cladding (125 μm) and buffer. n_1 —refractive index of the core, n_2 —refractive index of the cladding. To satisfy the conditions for total internal reflection $n_1 > n_2$.

the main focus of this paper is on measurement approaches that involve the detection of a measurand-induced modulation of the optical fibre's properties. The major hurdles faced by OFS technology in translation to, and adoption in, healthcare practice are outlined. Issues such as the careful consideration of the choice and robustness/longevity of chemically sensitive films, and the selection of technologies that will provide the most value to healthcare providers are discussed and future directions are proposed.

2. Introduction to OFS

Light propagates in the core of an optical fibre via total internal reflection with relatively low losses. This allows the transmission of information over long distances. The first working fibre optic data transmission system in 1965 [4] was demonstrated 100 years after the first demonstration of the concept of light propagation inside a medium via total internal reflection as a 'light fountain' [5]. Since then, the potential of light propagation inside a medium has been recognized and has resulted in numerous ideas for practical implementation, in areas ranging from imaging to high power light transmission. The main application nowadays is long distance high speed communication, facilitated by the reduction of transmission losses to as low as 0.2 dB km⁻¹ [6]. Owing to the unique properties of optical fibres, mainly their small size, no interference with electromagnetic radiation and prospect for remote sensing, the optical fibre has found niche applications in sensing.

A standard single mode optical fibre used in telecommunication, illustrated in figure 1, typically consists of three layers; a silica core of diameter of the order of microns (typically 2–10 μm) and doped with a material such as germanium to increase its refractive index (RI), a pure silica cladding of diameter 125 μm and a buffer coating that does not play a role in light guiding, but protects the fibre from mechanical damage and provides mechanical robustness. Optical fibres can also be made using materials such as plastic [7], chalcogenide [8] glasses or a combination of materials, where the core and cladding are of different composition. For

example, optical fibres having silica core and plastic cladding are commercially available [9]. Depending on the core size, wavelength of operation and difference in refractive indices between the core and the cladding, an optical fibre can operate in a single mode or a multimode regime. In the former, the profile of the light energy distribution across the core of the optical fibre is Gaussian, while in multimode fibre the profile is more complex [6].

Optical sensors detect changes in optical parameters that depend upon the physicochemical parameters of the investigated environment. Optical fibres offer a convenient method for the implementation of optical sensing, by directing light to, and collecting light from, the measurement region, so called extrinsic sensors [10] or by using the fibre itself as the transducer, so called intrinsic sensors [11]. In general, OFS operate by measuring changes in light propagation caused by external stimuli ranging from physical parameters (strain, pressure, temperature) to biochemical parameters (analyte concentration, chemical composition).

OFS offer several advantages over conventional sensor technologies [11, 12]. They are not susceptible to electromagnetic interference, they can survive harsh environments and tolerate high temperatures. They are biocompatible and are readily multiplexed, allowing the simultaneous monitoring of a number of measurands. They can be used for remote monitoring of the environment because of the low attenuation that is a property of light propagation in telecommunications grade single mode optical fibres. Optical fibre based measurement techniques have attracted a great deal of attention in a diverse range of applications such as structural monitoring, resin flow and curing, railway and aerospace, chemical and biological sensing, environmental monitoring and medical diagnosis. The variety of designs and measurement schemes that may be employed using optical fibres provides the potential for the creation of highly sensitive and selective sensors for deployment in real environments.

Since the main application of optical fibres is in communications, they are designed in such a way that minimizes influence of the external medium on the light (hence information) propagating inside the optical fibre. For efficient operation of OFS, however, the influence of the external medium should be maximized. This can be achieved using different optical fibre processing methods which frequently utilize interaction of the evanescent field with the external medium. The following sub-sections introduce the basic principles of the various configurations of OFS.

2.1. Cladding removed evanescent wave (EW) OFS

Perhaps the simplest way to achieve direct interaction of light with the medium surrounding the optical fibre is through the removal of the cladding to allow access to the EW, as illustrated in figure 2.

A change of the optical properties of the surrounding medium, for example, RI or spectral absorption, will lead to modulation of the light propagating in the optical fibre. This fibre modification facilitates EW spectroscopy [13], which is a highly sensitive and powerful technique that is used to

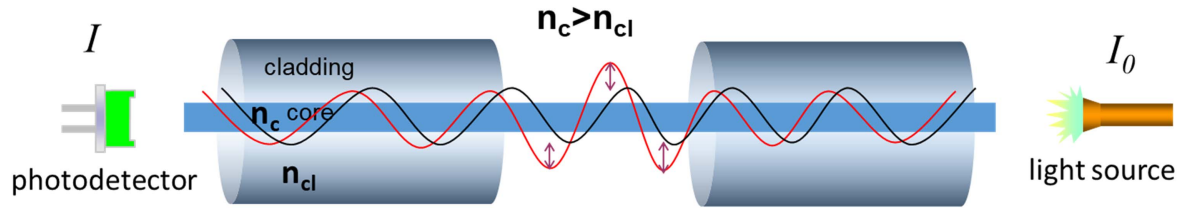


Figure 2. Schematic illustration of an evanescent wave based OFS with removed cladding.

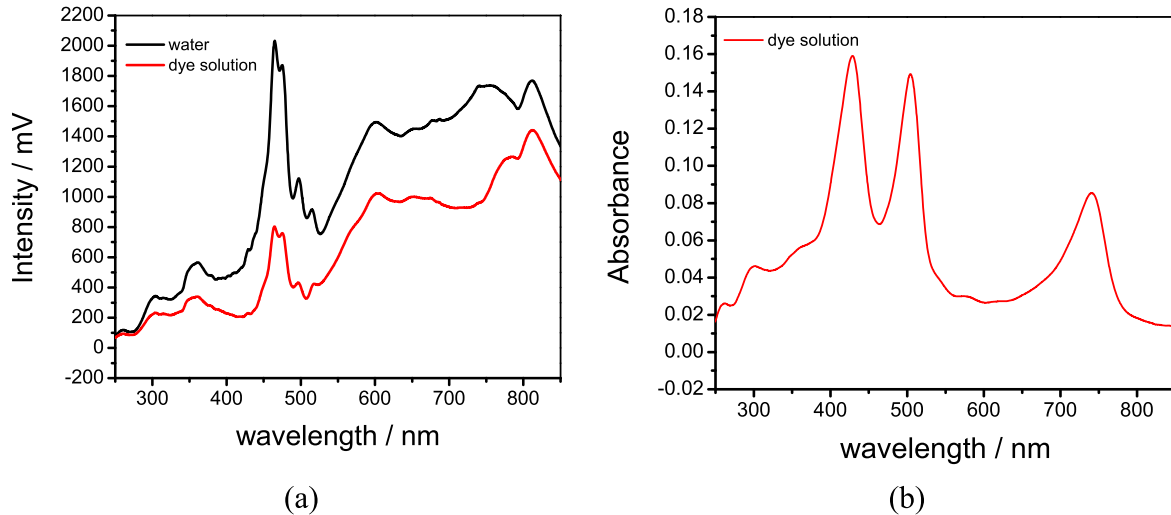


Figure 3. (a) Transmission spectrum of a hard-clad multimode silica optical fibre with the plastic cladding removed before (black line), and after (red line) immersion into a porphyrin dye compound; (b) absorption spectrum calculated from (a). Reproduced with permission from [13].

measure quantitatively and qualitatively the chemistry of the environment surrounding the optical fibre. The intensity of the EW decays exponentially with the distance from the interface between the fibre core and the surrounding environment. The penetration depth (d_p) of the EW is described by:

$$d_p = \frac{\lambda}{2\pi(n_{\text{eff}}^2 - n_s^2)^{1/2}}, \quad (1)$$

where λ is the wavelength of light in free space, n_s is the RI of the surrounding environment and n_{eff} is the effective RI of the mode guided by the optical fibre [10].

The absorption spectrum of the medium surrounding the fibre influences the attenuation of the EW, and thus of the mode, according to the Lambert–Beer law:

$$\frac{I}{I_0} = c^* \alpha^* L, \quad (2)$$

where α is the molar extinction coefficient, c is the concentration of the absorbing substance, L is the path-length that light travels through the sample and I_0 and I are the light intensities at the input and output of the optical fibre, i.e. before and after interaction with the absorbing substance, respectively.

In its simplest form, coupling the output from a broadband optical source into the proximal end of the fibre and observing the transmitted light by coupling the output from the distal end to a spectrometer will allow the spectroscopy of the surrounding medium to be measured. An example of the

use of EW spectroscopy, undertaken using a hard-clad multimode silica optical fibre with a section of the plastic cladding removed, to measure the absorption spectrum of a porphyrin dye compound is shown in figure 3 [13].

A variation of this type of OFS involves the creation of a ‘U’ shaped bend in a section of multimode optical fibre [14]. Bending the fibre causes the EW to extend further into the surrounding medium, increasing the interaction between the EW and the measurand [14]. There is also an implementation advantage as the source and detector are positioned on the same side of the medium under investigation. It is also worth mentioning that the low attenuation of chalcogenide glasses in the infrared (IR) region (1–10 μm), where specific absorption features of organic molecules are located, makes the use of these fibres attractive for EW spectroscopy [15].

2.2. Tapered OFS

Access to the EW can be also gained via tapering of a relatively short section (of length ranging from sub-millimetre to tens of millimetres) of the optical fibre. A tapered optical fibre consists of a region of fibre with reduced and uniform diameter (the waist) that is bounded by conical sections where the diameter of the fibre changes to merge the tapered section with the unperturbed surrounding fibre, as illustrated in figure 4(a). Tapered fibres are fabricated by heating and stretching the optical fibre with the heat source being typically a flame or the output from a CO_2 laser. The optical properties of the tapered fibre waveguide are influenced by the profile of

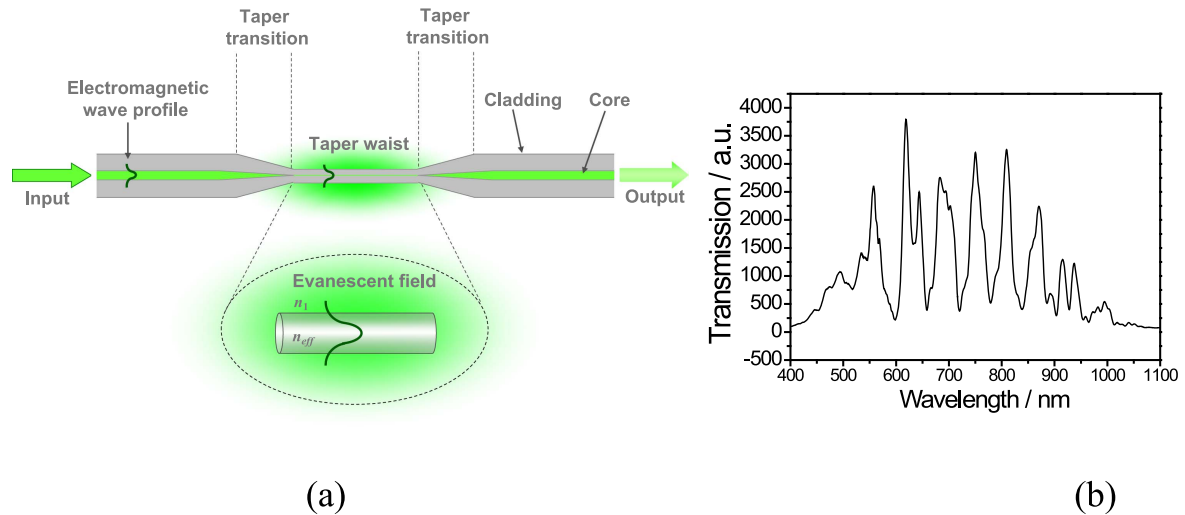


Figure 4. (a) Schematic illustration of the structure of a tapered optical fibre; and (b) a typical channelled transmission spectrum of a non-adiabatic taper with waist diameter of $10\ \mu\text{m}$ fabricated in an optical fibre with a cut-off wavelength of $670\ \text{nm}$. [16] [18 Apr 2012] Reprinted by permission of the publisher (Taylor & Francis Ltd, <http://www.tandfonline.com>).

the conical tapering sections, by the diameter of the taper waist and by the RI of the surrounding medium. The proportion of the power in the EW, and thus the interaction with the surrounding medium, increases with decreasing diameter of the taper waist, and with decreasing difference between the RI of the fibre and surrounding medium [16, 17]. Tapered optical fibres offer a number of attractive features for sensor development, including large evanescent fields, flexibility and compactness. In the case of a tapered optical fibre that is coated with a functional material, the properties of the waveguide are influenced by the optical thickness (product of the RI and geometrical thickness) of the coating.

Originally, tapered optical fibres were employed for the development of directional couplers, where two or more tapers are fused together, to provide efficient light coupling between fibres [18]. They have also found applications in sensor development [19], light amplifiers [20] and near and far field microscopy [21].

Optical fibre tapers are classified as adiabatic and non-adiabatic. In adiabatic configurations, the angle of the taper transition region is small (10^{-4} to 10^{-3} rad [22]) and the cylindrical symmetry of the optical fibre is retained (with taper ratio of taper diameter to initial diameter of the core (a/a_0) between 0.2 and 1 [22]), resulting in most of the optical power remaining in the fundamental mode [16]. The uniform transmission spectrum of adiabatic tapers facilitates their use for EW spectroscopy. In non-adiabatic tapers, the geometry of the taper is such that the fundamental mode is coupled into higher order modes. For non-adiabatic tapers of diameter less than $10\ \mu\text{m}$, the linearly polarized, LP_{01} , mode of the single mode fibre generally couples to the hybrid, HE_{11} and HE_{12} , modes of the tapered waist [23]. Interference effects in recombination of the excited modes at the 2nd tapering section introduce channelled spectrum features into the transmission spectrum, the wavelengths of which are sensitive to differential changes in the effective index of the modes, which arises from the different penetration depths of

their evanescent fields. This has been exploited to allow measurements of the RI of the surrounding environment or in the RI of chemically sensitive material deposited onto the surface of the tapered section of fibre.

Tapered optical fibres have been exploited as sensor platforms for a variety of applications [24–26]. There are two approaches that are used to exploit the interaction between the EW and the surrounding medium. The first involves the measurement of the attenuation of light propagating through the tapered region, which is influenced by both the spectroscopy and RI of the surrounding medium [15]. The second concerns the influence of the surrounding medium on the effective refractive indices of the modes propagating through the taper, which can be probed interferometrically, as described above, or by using mode coupling devices such as in-fibre gratings [27], surface plasmon resonances and lossy mode resonances [28].

2.3. Interferometers

Optical interferometry offers highly sensitive platforms for sensor development. The non-adiabatic tapered optical fibres described in the previous section are an example of a modal interferometer (MI). Other approaches include in-fibre gratings, regions of core mismatch and directional couplers [29]. Optical fibre MI rely upon the creation of a region where energy is coupled into two modes of the fibre. The modes then propagate along the sensing region of the fibre with different effective refractive indices and respond to the measurand differently.

Fibre optic MI are based on the interference between higher order and fundamental modes, which leads to a sinusoidal channelled transmission spectrum containing fringes described in section 1.2. The phase of the fringes of the spectrum depends on the difference in the optical path lengths of the interfering modes, according to [29]:

$$\varphi = \frac{2\pi}{\lambda}(\delta n_{\text{eff}})L, \quad (3)$$

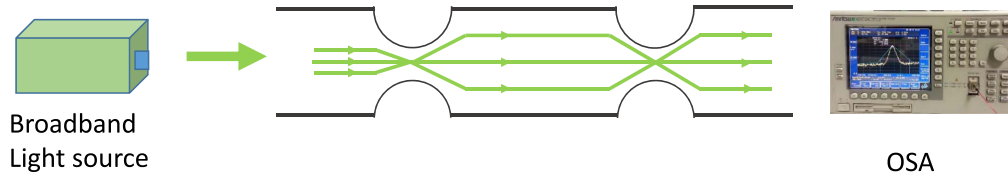


Figure 5. Schematic illustration of an optical fibre modal Mach-Zehnder interferometer [29].

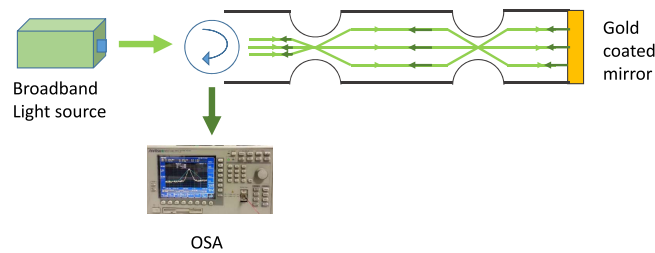


Figure 6. Schematic illustration of an optical fibre modal Michelson interferometer.

where λ represents the wavelength, L is the centre-to-centre distance between two coupling elements and δn_{eff} is the difference in refractive indices between the higher order and fundamental modes [29]. As the evanescent fields of modes of different order extend different distances into the surrounding medium, changes in the optical properties of the medium will influence the modes' effective refractive indices differentially, causing changes in the phase of the MI and of the channelled spectrum.

MI with configurations akin to the Mach-Zehnder interferometer (MZI) and Michelson interferometer (MchI) can be implemented in optical fibres. In the context of optical fibre tapers, as discussed in section 2.2, an MZI can be realized by fabricating a non-adiabatic taper of diameter $<10 \mu\text{m}$, in which two modes are excited at the first taper transition, which propagate with different effective refractive indices and which interfere at the second taper transition. External stimuli cause changes in the effective indices of the modes and thus induce a phase change in the channelled spectrum, figure 4(b) [26, 30]. An optical fibre MZI can also be created between two identical non-adiabatic tapers as shown in figure 5 [29]. The first taper couples the core mode to higher order cladding modes, while second recombines these modes to interfere and create the channelled spectrum. Changes in environmental parameters, such as temperature or RI, around the section of fibre separating the two tapered regions will induce a phase change that will result in a shift of the interference features of the spectrum. Optical fibre MZIs can also be implemented using coupling elements in the form of in-fibre gratings, regions of core mismatch and directional couplers [29].

In an example of an optical fibre MchI, illustrated in figure 6, the non-adiabatic taper couples the core mode to higher order cladding modes, which are reflected at the gold coated tip of the optical fibre and are recombined at the same taper to produce interference fringes. Again, changes in

environmental around the section of optical fibre separating the taper and the gold coated tip will induce a phase change that will result in shift of the interference features of channelled spectrum. For the same physical length of the interferometer, a MchI will exhibit higher sensitivity as light traverses the sensing region twice. MchI can also be implemented using coupling elements in form of in-fibre gratings and regions of core mismatch [29].

These types of interferometers can be interrogated by measuring the wavelength shifts of the features in the channelled spectrum or by recording an amplitude change at a fixed wavelength, table 1. Another example of an interferometric OFS is the so called Fabry-Perot interferometer (FPI), which consists of a cavity formed between two reflectors, as illustrated in figure 7. This cavity can be formed by a gap between two fibres, or between the tip of the fibre and a membrane (figure 7(a)). Alternatively, a thin film can be deposited at the tip of the fibre to form an FPI, where the interface between the fibre tip and the film forms one reflector and the interface between the film and the surrounding medium forms the second mirror.

The total reflected power (P_R) for thin film FPI case is described by [29]:

$$P_R = R_1 + (1 - A)^2(1 - \alpha)^2(1 - R_1)^2 \cdot R_2 \cdot e^{-4\alpha L} + 2(1 - A)(1 - \alpha)(1 - R_1)\sqrt{R_1 R_2} \cdot e^{-2\alpha L} \cos\left(\frac{4\pi\eta_f L}{\lambda}\right), \quad (4)$$

where $R_1 = [\eta_{\text{fibre}} - \eta_f / \eta_{\text{fibre}} + \eta_f]^2$ is the Fresnel coefficient at the interface fibre-film and $R_2 = [\eta_f - \eta_{\text{air}} / \eta_f + \eta_{\text{air}}]^2$ is the Fresnel coefficient at the interface film-air; α is the transmission loss factor inside the cavity (absorbance) and A is the loss coefficient at the first interface fibre-film; η_{fibre} is the RI of the fibre, η_{air} is the RI of the air, L is the physical thickness of the nano-coating and η_f is the effective RI of the

Table 1. Summary of the measurands and measured light parameter monitored/detected by different types of OFS.

Type of the sensor	Measured light parameter	Units	Measurand
Cladding removed evanescent wave	Intensity	dB, %,	Concentration, absorption
Tapered	Intensity, wavelength shift	dB, %, nm	Concentration, RI, absorption, pressure, temperature, strain
Fibre Bragg grating	Wavelengths shift, Intensity	dB, %, pm	pressure, temperature, strain
Long period grating	Wavelengths shift, Intensity	dB, %, nm	Concentration, RI, absorption, pressure, temperature, strain
Interferometers	Wavelengths shift, Intensity, phase	dB, nm, %, degrees	Concentration, RI, absorption, pressure, temperature, strain

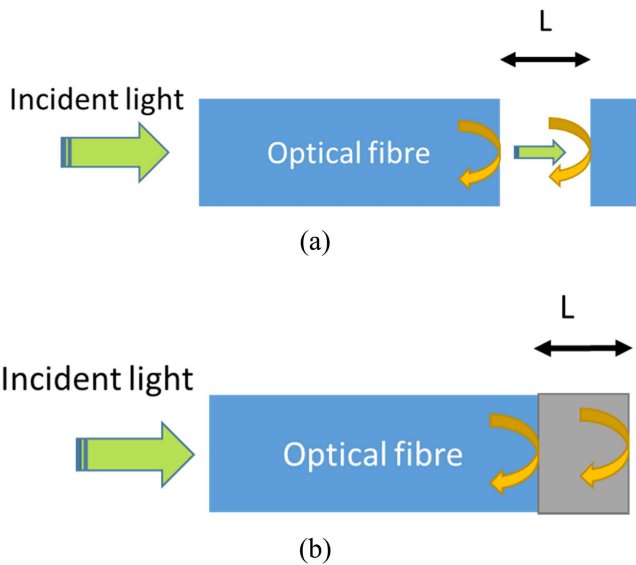


Figure 7. Schematic illustration of a Fabry–Perot interferometer formed (a) by a gap between two optical fibres (or between the fibre end and a membrane); and (b) by depositing thin film at the tip of the optical fibre.

film. A change in either the RI of the cavity or its length will modulate the reflected power, which can be used to detect the measurand that modulates the coating’s parameters.

2.4. Grating based OFS

Fibre optic devices based on grating structures inscribed into optical fibres have been investigated extensively for sensing applications [31]. An optical fibre grating consists of a periodic modulation of the propagation constants of the modes of the optical fibre, typically induced by a modulation of the RI of the core of the fibre by exposure to a spatially modulated intensity pattern from a UV or femtosecond laser [31]. In the case of a grating that has a period on the order of the wavelength of light (around 1 μm), a so called fibre Bragg grating (FBG), the grating acts to couple the forward propagating mode to a backward propagating mode of the core at a wavelength that satisfies the Bragg condition, which is dependent on the period of the grating and the effective RI of the propagating mode, figure 8. An FBG is viewed as a wavelength selective mirror, which reflects a narrow band of

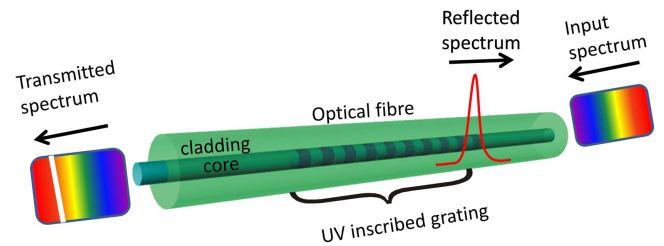


Figure 8. Schematic illustration of an FBG (grating period 100 s nm) and LPG (grating period 10 s to 100 μm).

wavelengths back along the optical fibre while transmitting all other wavelengths. The reflected Bragg wavelength is governed by [31, 32]:

$$\lambda_{\text{Bragg}} = 2n_{\text{eff}}\Lambda, \tag{5}$$

where n_{eff} is effective RI of the mode propagating in the core and Λ is the period of the grating.

The Bragg wavelength is sensitive to parameters that influence the period of the grating and RI of the fibre, typically strain and temperature [31, 32]. The wavelength-encoded nature of the sensor offers a number of advantages, not least the ability to multiplex a serial array of FBG sensors in a single optical fibre by ensuring that each has a different period, and thus a different Bragg wavelength. To sensitize the Bragg wavelength to the surrounding RI, the fibre has to be polished, etched or tapered to allow the EW to interact with the surrounding medium. The interaction of the EW with the surrounding medium influences the effective index of the propagating mode, resulting in changes in the Bragg wavelength, and, as the attenuation of the taper is dependent upon the surrounding RI, changes in the reflected power. The total wavelength shift ($\Delta\lambda$) due to strain (ε) and temperature change (ΔT) can be approximated by equation (6) [31, 32].

$$\Delta\lambda = \lambda_{\text{Bragg}}[(1 - P_e)\varepsilon + ((1 - P_e) \cdot \alpha + \xi)\Delta T], \tag{6}$$

where P_e the photoelastic is constant, ξ is the thermo-optic coefficient of the optical fibre and α is the thermal expansion coefficient [31, 32].

Tilted FBGs (TFBGs), where the grating planes fabricated such that they are inclined with respect to the axis of the fibre, can be used to measure the changes in the surrounding RI without the need for further modification of the fibre. TFBGs, in addition to coupling light to a backward propagating mode

at the Bragg wavelength, also couple light to forward propagating modes of the cladding, creating further spectral features. The interaction of the cladding modes' EWs with the surrounding medium changes their effective refractive indices, resulting in changes to the wavelengths of the cladding mode coupling features (the Bragg wavelength is unchanged) [33].

In contrast to FBGs, a long period grating (LPG) typically has a period in the range $100\ \mu\text{m}$ to $1\ \text{mm}$ and couples light from the core mode to a discrete set of co-propagating cladding modes, also shown in figure 8 [13]. As the cladding modes suffer high attenuation, the transmission spectrum of an LPG is characterized by a series of resonance bands, each corresponding to coupling to a different cladding mode. The resonance wavelengths are dependent on the product of the period of the LPG and the difference between the core and cladding mode indices, governed by [34]:

$$\lambda_i = (n_c - n_{\text{clad}}^i)\Lambda, \quad (7)$$

where Λ is the period of the grating, n_c is the RI of the mode propagating in the core, and n_{clad}^i is the effective index of the i th axially symmetric and linearly polarized cladding mode [34, 35].

As a result of the interaction of the EW of the cladding modes with the surrounding medium, the resonance wavelengths are inherently sensitive to changes in the surrounding RI, and to the optical thickness of nanoscale coatings deposited onto the cladding. This makes LPG sensors ideal candidates for development of refractometers and biosensors. In biosensor applications, since the LPG is sensitive to both bulk (due to concentration change) and surface (due to binding events) RIs, special care needs to be taken to address this difference. The different ways of addressing this and enhancing the sensitivity of LPGs in bio-sensing applications have been thoroughly described in recent paper by Chiavaioli *et al* [3].

LPGs fabricated in standard single mode optical fibres offer inherent sensitivity to a number of parameters, predominantly strain, temperature, curvature and surrounding RI [34]. The temperature sensitivity of the central wavelength (λ_i) of the LPG can be calculated using equation (8) [36] and the sensitivity to the variation of the surrounding RI (n_3) can be calculated using equation (9) [37],

$$\frac{d\lambda_i}{dT} = \frac{d\lambda_i}{d(\delta n_{\text{eff}})} \left(\frac{dn_c}{dT} - \frac{dn_{\text{clad}}^i}{dT} \right) + \Lambda \frac{d\lambda_i}{d\Lambda} \cdot \frac{1}{L} \frac{dL}{dT} \quad (8)$$

$$\frac{d\lambda_i}{dn_3} = \frac{d\lambda_i}{dn_{\text{clad}}^i} \cdot \frac{dn_{\text{clad}}^i}{dn_3}, \quad (9)$$

where L is the length of the LPG, Λ its period, $\delta n_{\text{eff}} = n_c - n_{\text{clad}}^i$ (differential effective index). The cross-sensitivity to strain is not considered in this treatment since material (strain-optic and Poisson's effect) and waveguide (change of the grating period) contributions to strain sensitivity can cancel each other out having opposite signs [36, 37]. The phase matching condition described by equation (7) contains a turning point at which it has been demonstrated [38–40] that the sensitivity of the attenuation band to perturbation of the surrounding environment is at its maximum, i.e. there is optimum sensitivity when the LPG is

fabricated with a period such that the coupling of light to the cladding mode occurs near to or at the phase matching turning point [41]. Among the various types of OFS, those based on optical fibre gratings offer wavelength-encoded information that overcomes the referencing issues associated with intensity based approaches.

2.5. Summary

The properties of the OFS described in this section are summarized in table 1. According to the measurands, OFS can be broadly classified into physical, chemical and biosensors.

As mentioned in [3], it is often difficult to compare the performance of the different OFS even when same measurand is measured, as authors usually provide limited information, typically stating only the units of sensitivity, which differ when different principles of operation of the sensors is employed (table 1). For example, sensitivity to temperature measured using an FBG will be reported in $\text{pm } ^\circ\text{C}^{-1}$ while that measured by an interferometer be reported in $\text{rad } ^\circ\text{C}^{-1}$ or $\text{dB } ^\circ\text{C}^{-1}$, which makes comparison of sensors in terms of sensitivity meaningless. There is a need for the optical sensor community to develop standardized units of measurements to allow comparison of the performances of different types of OFS. Perhaps the performance of the sensor can be expressed in terms of a figure of merit that will allow this comparison—this could well be the range, resolution/accuracy or limit of detection (LoD) of the particular measurand, as this takes into account standard deviation. This discussion, however, is beyond the topic of the current review paper and readers are referred to [3] for a detailed discussion of OFS metrology.

3. Physical measurands in healthcare

3.1. Temperature

Temperature is one of the vital signs and is a crucial and routinely monitored parameter in medicine that is measured using a variety of technologies [42] in all clinical settings, including surgeries, oncology treatment and intensive care units [43]. In healthcare, the temperature sensing requirements are application dependent, but generally a temperature range of $35\ ^\circ\text{C}$ – $45\ ^\circ\text{C}$ with a resolution of at least $0.1\ ^\circ\text{C}$ is required [44]. The required response time of the temperature sensor is also application dependent [2]. For some thermal treatment procedures, such as high-intensity focused ultrasound ablation, the coagulative temperature ($43.5\ ^\circ\text{C}$ – $57.0\ ^\circ\text{C}$) is reached within less than 30 s [45], while for laser ablation this can lie between 5 and 15 min [45].

Typically, OFS will be deployed to measure temperature when immunity to electromagnetic interference or electrical insulation are required [44, 46], such as during magnetic resonance imaging (MRI) or radio frequency (RF) treatment [46–48]. OFS temperature sensors exploit a range of transduction principles, such as temperature dependent fluorescence lifetime [49–52], Rayleigh scattering (change in the amplitude of the back-reflected signal with temperature) [53] and thermal

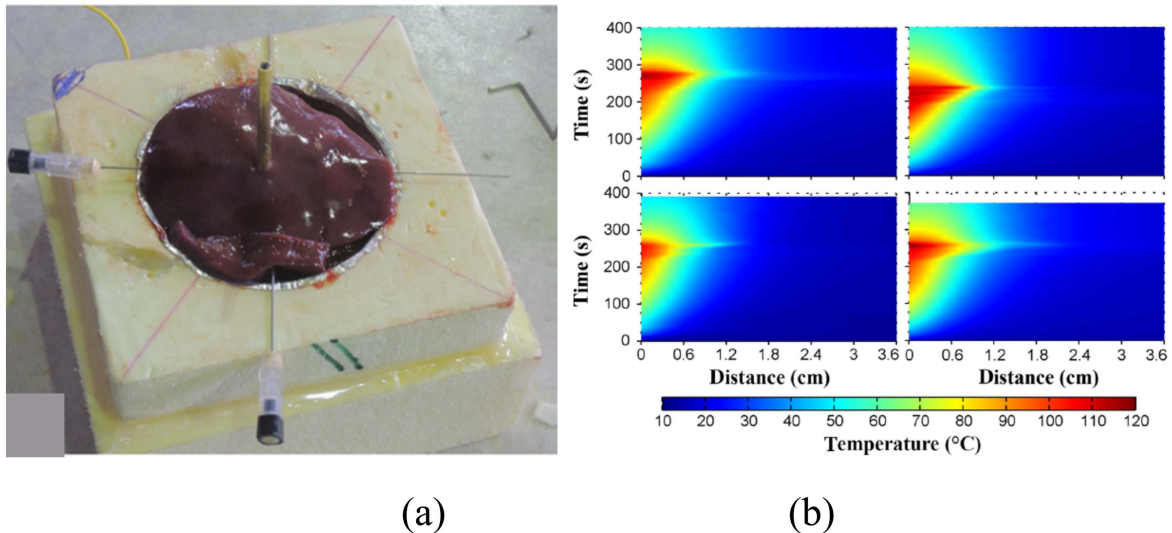


Figure 9. (a) One-dimensional (1D) axisymmetric experimental chamber—the optical fibre is inserted into the tissue through medical needles; and (b) average temperature space–time evolution for each repeated experiment. Reproduced with permission from [62].

Table 2. Summary of key parameters of optical fibre temperature sensors.

OFS	Sensitivity	Resolution	Range	Response time	Reference
Fluorescence	$0.5 \mu\text{s } ^\circ\text{C}^{-1}$	$\pm 0.50 \text{ } ^\circ\text{C}$	$20 \text{ } ^\circ\text{C} - 80 \text{ } ^\circ\text{C}$	— ^a	[59]
FBG	$27 \text{ pm } ^\circ\text{C}^{-1}$	—	$20 \text{ } ^\circ\text{C} - 80 \text{ } ^\circ\text{C}$	100 ms	[60]
FPI	$0.19 \text{ nm } ^\circ\text{C}^{-1}$	$0.34 \text{ } ^\circ\text{C}$	$25 \text{ } ^\circ\text{C} - 80 \text{ } ^\circ\text{C}$	$67 \text{ } ^\circ\text{C/s}^{\text{b}}$	[61]
Rayleigh scattering	$10 \text{ pm } ^\circ\text{C}^{-1}$	$0.1 \text{ } ^\circ\text{C}$	$20 \text{ } ^\circ\text{C} - 46 \text{ } ^\circ\text{C}$	1 s	[62, 63]

^a No information available.

^b This is the rate of temperature change that sensor can measure, rather than the response time.

expansion and the thermo-optic effect in FBGs [54–56], LPGs and FPIs [57, 58]. Table 2 summarizes key parameters of optical fibre temperature sensors [2].

In addition, optical fibre temperature sensors, especially those based on gratings and Rayleigh scattering, offer a prospect for multiplexed or distributed temperature sensing, allowing the generation of a heat map of the area of interest [27, 62, 64, 65]. Figure 9 shows an example of the temperature distribution measured inside liver tissue (figure 9(a)) using a Luna OBR4600 optical fibre distributed temperature sensor (DTS), measuring changes in the Rayleigh back scattering signal in the optical fibre, during an RF ablation procedure [62]. The equipment was configured such that measurement time of 1 s for the entire fibre length (<20 m) and choosing an accuracy estimated as $0.5 \text{ } ^\circ\text{C}$, a minimum spatial resolution of $200 \mu\text{m}$ in real time (and $20 \mu\text{m}$ in post-analysis with data processing) was achieved. The performance of the DTS Luna Rayleigh back scattering system depends on a tight trade-off between accuracy, spatial resolution, and sampling time. Analysis of the thermal maps verified that the spatial and temporal evolutions of the temperature were smooth and consistent with what would be physically anticipated [62]. The authors reported that measurements can be employed to investigate the physics of RF ablation and for the validation of ablation models. Results can be used for investigating the physics of thermal ablation, to

set the basis for distributed temperature monitoring and for the validation of models [62]. It has the potential to facilitate the adjustment of treatment to the specific biological and electrical properties of the tissue undergoing ablation.

Despite the commercial availability of OFS systems targeted at healthcare, based on various measurement principles, offered by FISO, LumaSense, Neoptix and OpSens, there are limited reports of *in vivo* use of OFS with animals or humans [2]. Fajkus *et al* [66] proposed a system based on FBGs for vital sign measurements (body temperature, heart rate and respiratory rate). The system consisted of 32 FBG sensors that were embedded into polymer to increase their temperature sensitivity. The FBGs were interrogated using a wide-spectrum SLED (1512.5–1587.5 nm and an output power of 1 mW) connected to spectrum analyser via a fibre optic circulator. The system was tested on 10 human volunteers, with the measurements showing good correlation with standard equipment routinely used in hospitals [66]. The main advantage of the system identified by authors was the design of the novel patient-friendly non-invasive measurement probe.

For applications such as cryo-ablation, OFS need to perform at temperatures down to $-180 \text{ } ^\circ\text{C}$ [67]. Samset *et al* [67] measured the temperature distribution using 10 wavelength division multiplexed FBG sensors. Adjacent sensor elements were separated by 6.5 mm and the external diameter of the probe was 1.25 mm. The median difference between

measured and estimated temperature was 3.03 °C, and the measurements provided valuable information for the development of models of cryo-ablation. Temperature maps as outlined in the work may be used for monitoring of cryo-therapy in order to increase clinical effectiveness.

Yoo *et al* [68] proposed respiration sensors based on thermo-chromic material deposited onto the tip of plastic optical fibre for respiratory monitoring inside an MRI system. Two types of non-invasive fibre optic respiration sensors were reported, one being a nasal-cavity attached sensor that could measure the temperature variation of air-flow using a thermo-chromic pigment. The other was an abdomen-attached sensor that measured the abdominal circumference change using a sensing component composed of polymethyl-methacrylate tubes, a mirror and a spring. The intensity of reflected light was changed by the variation of the distance between the mirror and the distal end of the plastic optical fibre according to abdominal movement. The authors verified that respiratory signals can be obtained with no detrimental effects on the magnetic resonance image.

Musolino *et al* [69] described a fluorescence based optical fibre temperature sensor based on rear earth glass deposited onto the tip of an optical fibre. The sensitivity was reported to be $0.005\ 258\ \text{K}^{-1}$ over a temperature range of 22 °C–51 °C. The sensor was tested successfully *in vivo* by measuring the brain temperature of rats [69]. A comprehensive review of optical fibre temperature sensors and their applications in healthcare can be found in [2].

The temperature sensitivity of the light propagating through optical fibres compromises the sensing of other measurands, and hence temperature needs to be taken into account when measuring other parameters. This can be done either by developing temperature insensitive sensors [70, 71] or by measuring temperature independently to other measurand and subsequently compensating for its effect [72].

3.2. Pressure

Pressure in the human body is grouped into two categories, isotropic pressure, such as blood pressure and intracranial fluid pressure, and contact pressure such as intra vertebral pressure. Blood pressure, in particular, is a vital sign in the human body that is routinely measured during medical examinations and procedures [1, 73]. The pressure range of interest, however, is very wide, is dependent on the part of the body where the measurement is performed and is influenced both by external and internal factors [73]. The pressure in the human body at normal physiological conditions is typically divided into three levels [73, 74]:

- low pressure domain—between 0 and 10 mbar (1 mbar = 100 Pa \approx 0.75 mmHg); (capillaries, brain, urinary bladder, and muscular compartments)
- medium pressure domain—the values lie between 25 and 150 mbar (circulatory system including the heart)
- high pressure domain—the values can be as high as 180 mbar (load bearing structures like hips and knees) (135 mmHg).

At pathophysiological conditions, the pressure can vary significantly and range from -0.1 bar (-10 kPa, -75 mmHg) for intra-alveolar and intra-tracheal pressure to as high as 0.4 bar (40 kPa, 300 mmHg) for aortic and left ventricular pressure [74]. These requirements place constraints on optical fibre pressure sensors. Ideally, an optical fibre pressure sensor should be able to operate between 0.04 bar (-4 kPa, -30 mmHg) in the heart [75] to 10 bar (7500 mmHg) in bones and joints [76, 77] with a typical resolution of 1 mbar (0.75 mmHg) and accuracy of $<1\%$ [44]. In practice, however, the sensors will cover much narrower range to satisfy requirements of a particular application.

A variety of OFS can be used to measure pressure, such as intensity modulated, FBGs [78–80] and FPIs [81].

Intensity modulated pressure sensors were originally proposed for pressure measurements in 1960s [82] but, despite the simplicity of the design and its cost effectiveness, they have not found widespread application. There are two main designs, one based upon a movable reflectance membrane interfaced with the tip of the optical fibre such that the intensity of light reflected back into the fibre depends on the pressure [83, 84]. The second relies upon bending losses, where the pressure dependent bend will induce loss in light propagation inside the optical fibre [85]. The main drawback of these approaches is their reliance on the measurement of intensity, which can be influenced by a wide range of parameters including light source fluctuation, changes in the reflectivity of the membrane (due to temperature or oxidation effects) and bending of the fibre [86].

The inherent sensitivity of single mode silica optical fibre FBGs to hydrostatic pressure is not very high ($0.304\ \text{pm bar}^{-1}$ ($4.05 \times 10^{-4}\ \text{pm mmHg}^{-1}$)) [87]. Increasing the pressure sensitivity is typically achieved by transducing the pressure into a strain acting along the axis of the fibre by appropriate packaging. One of the approaches consists of attaching the FBG to a flexible diaphragm either orthogonally or in the diaphragm plane in areas where the strain is maximal. Another approach involved the packaging of the FBG sensor in a cylindrical assembly so that pressure sensitivity can be increased via mechanical amplification schemes [86]. Sensitivity can be enhanced to $270\ \text{pm bar}^{-1}$ ($0.36\ \text{pm mmHg}^{-1}$) when the FBG is embedded into a flexible patch that translates the transverse load into an axial strain measured by the FBG [88, 89].

Fabry–Perot sensors offer the highest sensitivity to pressure and can be implemented with great design flexibility [86]. A compact pressure sensor was developed by FISO [90], where the diameter of the sensor head was $125\ \mu\text{m}$ with standard range of ± 300 mmHg and system accuracy of ± 3 mmHg. A detailed review of optical fibre pressure sensors is beyond the scope of this paper, but more details of optical fibre pressure sensors can be found in recent reviews in [77, 81, 91]. Table 3 provides key parameters of optical fibre pressure sensors [91].

Optical fibre pressure sensors have been trialled in both *ex vivo* and *in vivo* applications in various areas of healthcare, including gastroenterology, cardiology, neurology and urodynamic. The review by Poeggel *et al* [1] summarizes comprehensively these applications. Optical fibres have also been

Table 3. Summary of key parameters of optical fibre pressure sensors.

OFS	Sensitivity	Resolution	Range	Response time	Reference
FBG	From 5.870^a pm bar ⁻¹ (7.8×10^{-3} pm mmHg ⁻¹) to 270 pm bar ⁻¹ (3.6×10^{-4} pm mmHg ⁻¹)	From 0.013 bar (9.75 mmHg) to 0.08 bar (60 mmHg)	0–50 bar	From 5.870^a pm bar ⁻¹ (7.8×10^{-3} pm mmHg ⁻¹) to 270 pm bar ⁻¹ (3.6×10^{-4} pm mmHg ⁻¹)	[88, 89, 91, 92]
FPI Intensity modulated	$0-3.8 \times 10^4$ mmHg — ^b	— ^b	–50 to 0.4 bar (300 mmHg)	(0–3.8) × 10 ⁴ mmHg 40 s	[91, 93–96] [84, 91, 97]

^a Comprehensive review on optical fibre pressure sensors with detailed sensor parameters can be find in [91].

^b No data available.

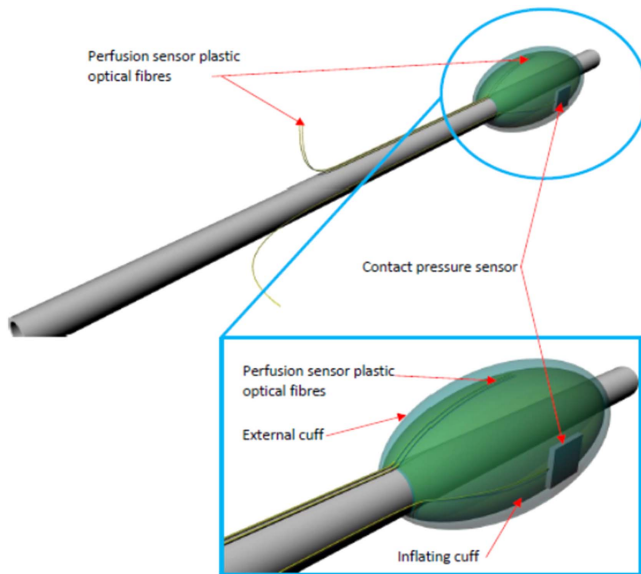


Figure 10. Fibre optic pressure and perfusion sensors bonded to the ETT cuff and then enclosed within an external cuff. Reproduced with permission from [100].

used for contact pressure sensing in applications in biomechanics and rehabilitation or at the interface between the medical device and tissue (e.g. sockets, bandages [77], in bone, dental biomechanics and as insole and amputee socket sensors). A number of applications were reviewed by Poeggel *et al* [1] and by Al-Fakih [77]. Here, more recent examples of *in vivo* pressure sensors applications are outlined.

OFS were applied recently to address an important problem known as medical device related pressure ulcers, which causes over a third of soft tissue damage in hospitals [98, 99]. Here, the optical fibre pressure sensor was based on an FBG embedded into a polymer patch with high sensitivity to contact pressure, which could be used to measure at the interface between a medical device and tissue [89, 100].

The Arkwright group [101, 102] has recently proposed an interesting approach to pressure sensing involving the use of FBG sensors entwined in a double helix, which allows real time, distributed sensing of pressure to be performed with inherent temperature immunity. The sensor can be used in compression bandaging and for *in vivo* colonic diagnostics [80]. Compression bandaging is a major approach in healthcare for the treatment of conditions such as venous leg ulcers and lymphoedema, where precise control of the applied pressure is essential. The FBG based sensors were blind tested on 46 humans with results showing a correlation to the target gradient of 93% [102].

One example of internal tissue damage that can occur is post-intubation laryngotracheal stenosis, which is caused by use of an endotracheal tube (ETT) during mechanical ventilation. It is a life threatening debilitating condition with a protracted course, typically requiring multiple complex surgical procedures. ETT is used in mechanical ventilations and consists of lumen that is used to deliver artificial air and an inflatable cuff that holds tube in place and ensures that there is

no leak of secretions into the lungs; figure 10. A sensorised ETT was developed with the aim of aiding a reduction in soft tissue damage and improving design of future devices. Optical fibre sensing was used to monitor both cuff contact pressure (via a packaged FBG) and tissue perfusion (via reflectance photoplethysmography (PPG), which detects blood volume changes in the microvascular bed of tissue). The monitoring system was used successfully in an animal study, demonstrating reliable measurement of contact pressure and perfusion (PPG) [100]. Both the FBG and the perfusion sensor were bonded to the outside of the cuff and an additional outer cuff was bonded to the ETT in order to enclose the sensors and inner cuff (figure 10).

The FBG sensor incorporated into the ETT was interrogated using a commercially available system (Smartsan, Smart Fibres Ltd, Bracknell, UK), which uses a tuneable laser diode to provide swept wavelength illumination of the FBG. This wavelength shift is related to the applied pressure after compensating for temperature by subtracting readings from an FBG that was not embedded into the patch. Perfusion was measured using reflectance PPG and the recorded data sent to a laptop for further processing. The device was tested on six pigs to investigate whether pressure and blood flow could be monitored reliably *in vivo*. The results are shown in figure 11. It is interesting to note that the FBG could measure changes in respiration due changes in the contact pressure between the sensor and trachea (figure 11(a)). The measurements also revealed that high cuff pressures occluded the blood flow, such that the pulsatile signal could not be observed at high pressure but returned when pressure was reduced. The sensor demonstrated high quality reliable PPG signal return from tissue when the cuff was brought into optimum contact with the trachea.

3.3. Respiratory and heart rate and blood flow measurements

The response of an FBG to strain can be used to measure the periodic mechanical movement of the chest wall caused by breathing or cardiac contractions and hence monitor respiration and heart rate [103]. Heart rate can be measured using FBG sensors via the detection of the pressure pulse waveform (PPW) generated by the heart that travels through the human body [104]. The principle of operation of such a sensor is based on the detection of the change of the Bragg wavelength of an FBG placed close to an artery by the PPW travelling in the artery. A number of configurations have been demonstrated, including adhering the FBG to a silicone diaphragm, which in turn is adhered to a hollow box [105], a portable pen-like OFS [106], and a lever amplification mechanism [104].

Similar principles may be used to measure respiratory rate, where movement of the chest generates a strain acting on FBG [103] or LPG [107, 108] sensors. Both LPGs and FBGs can be embedded into textiles to create wearable unobtrusive sensor devices [109, 110]. OFS have been used extensively in monitoring respiration in MRI scanners and a useful review is provided in [111].

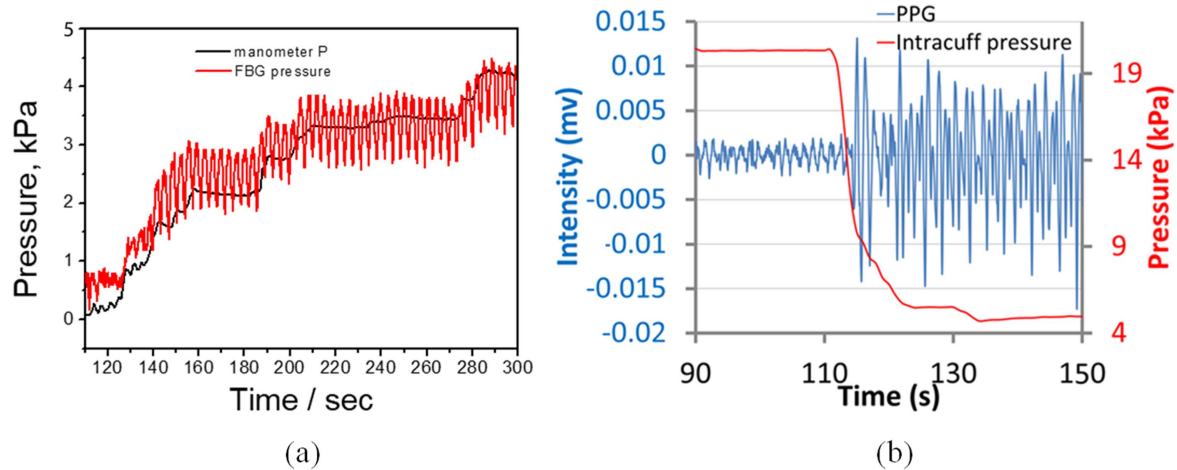


Figure 11. Comparison of the pressure measured by an FBG sensor at the interface between cuff and trachea and a manometer, which measured intracuff pressure. The oscillation in the contact pressure is due to the mechanical ventilation, which caused a change in contact pressure as the lungs expanded and contracted. (b) Reflectance PPG with a change in cuff pressure. After reducing the pressure the PPG signal returns. Reproduced with permission from [100].

The other physical parameter that is routinely measured in clinical settings is blood flow [112]. Optical fibre Doppler flowmetry is used routinely for blood flow measurements [113]. The role of the optical fibre in this measurement is to deliver to, and collect light from, the measurement point. Optical fibre velocimeters have been reviewed in detail in [114]. The role of the optical fibre in these measurements is simply to deliver and collect light to and from the measurement point and will not be discussed in further in this review.

4. Biochemical measurands in healthcare

In addition to high sensitivity and low limits of detection, one of the crucial sensor parameters in biochemical measurements is selectivity, which is the ability to detect the particular measurand of interest in the complex matrix of other, often interfering, measurands (both physical and biochemical). The optical fibre RI sensing platforms described in section 1 are not selectively sensitive to a particular chemical measurand (analyte). There are two approaches that are used to imbue OFS with a selective response. The first is based on EW spectroscopy in which interaction between EW and analyte allows direct analysis of the spectroscopy of an analyte [115–117], as described in section 1.1. This approach, however, requires special optical fibres made of material that is transparent in the IR wavelength range, [118] where biochemical analytes have rich absorption features [119]. These materials can be chalcogenide glasses, fluoride or silver halide glasses [118]. At this stage, the use of these special optical fibres in healthcare is limited because of the potential toxicity of chalcogenide glasses [120] and further research is required to better understand their behaviour in biological systems.

The second approach involves the indirect measurement of the analyte, whereby a chemically sensitive functional coating, which changes its optical properties when it comes

into contact with the analyte, can be deposited onto the surface of the optical fibre. Using appropriate OFS sensing platforms, the changes in the characteristics of the coating can be transduced to a change in the properties of the light propagating in the fibre. Analysis of the optical fibre's transmission spectrum can then provide quantitative and qualitative information on the chemical species under examination. The use of chemically sensitive coatings means that the operating wavelength of the sensor is defined by the coating properties, rather than by the absorption spectrum of the analyte, which can be advantageous. OFS based on this approach offer the prospect for the development of cheap and compact devices, due to the combination of low cost light emitting diodes and photodetectors. The sensitivity of the device is dependent on the length of the sensing area and, for efficient operation, coating materials with strong optical absorption features should be selected [121]. This section focuses on the functionalisation of OFS for the development of biochemical sensors, as this is an area of considerable research interest and innovation. Although the technology is maturing there has been little work on its use *in vivo*.

4.1. Chemical OFS

The detection of chemical compounds in the human body can be conducted in the gas phase, analysing exhaled gases in the breath or gases emitted through the skin, or in the liquid phase, in samples such as urine, saliva, sweat, tears and blood.

4.1.1. Detection in gas phase. Gaseous compounds excreted from the human body (biomarkers) reflect certain metabolic conditions as well as the blood gaseous content, which offers a possibility for the development of non-invasive diagnostics [122]. The classification of bacteria related to human diseases [123, 124], urinary tract infections [125] and further progress to metabolic disorders such as diabetes [126] or renal dysfunction [127] has been achieved by monitoring biomarkers. Further,

Table 4. Summary of optical fibre based ammonia sensor parameters.

Sensor type	Sensitive element	Limit of detection (LoD)/lowest measured concentration (LMC)	Response time	Reference
Cladding removed evanescent wave	Universal pH indicator	10 ppm(LMC)	5 min	[144]
	Bromocresol purple/bromocresol green, dip coating sol-gel	9 ppm (LMC) 0.014 dB ppm ⁻¹	8 s	[145]
	Bromocresol purple, sol-gel	145 ppm (LMC)	10 s	[146]
Reflection type	TSPP	6 ppm	15 s	[13]
	ZrO ₂ /PSS Nano-assembled	1 wt% (LMC)	Minutes	[148]
Lossy mode resonance	Oxazine 170 perchlorate	200 ppm (LMC)	—	[149]
	Titanium dioxide containing TMPyP	0.1 ppm (LMC)	30 s	[143]
Grating based	PDDA/TSPP	0.67 ppm (LoD)	—	[147]

renal failure in rats [128] and lung cancer detection in people [129] have been achieved using the breath sniffing method and using arrays of appropriately modified chemo-resistors.

Despite the interest and success in characterizing human odours, only few methods have the potential to be employed in clinical practice. Most of these methods have been used for monitoring the presence of gases such as CO, NO, isoprene [130], acetone [131], and ammonia [132] in human breath.

CO₂ and oxygen are two gases that are routinely measured in clinical settings [133]. OFS can be used to measure both of these gases via the simultaneous excitation of two fluorescent pH sensitive indicators with well-separated emission bands [134]. It was reported that oxygen can be continuously monitored in the 0–200 Torr (0–26.6 kPa) range with ± 1 Torr accuracy and that CO₂ can be monitored in the 0–150 Torr (0–20 kPa) range with ± 1 Torr accuracy. The accuracy is higher at low partial pressure, so that the detection limits are defined at ~ 0.5 Torr in both cases [134].

In clinical settings, IR spectroscopy (capnography) is used to detect CO₂. In demonstrations of CO₂ OFS, pH sensitive indicators are usually used. Kole *et al* measured breath-to-breath CO₂ and oxygen using an optochemical oxygen sensor, exploiting the measurement of the quenching of the intensity of photoluminescence of the dye platinum (U)-octaethylporphyrin-ketone [135]. One of the issues with dye based OFS is the lifetime, as the dye tends to leach and thus the coating loses its sensitivity. An optical fibre CO₂ sensor based on an LPG coated with metal organic compounds (HKUST-1) to detect CO₂ was proposed recently [136]. The sensor operated in the range of 500–40 000 ppm of CO₂ with the LoD of 401 ppm.

Ammonia is one of the major metabolic compounds and the importance of its detection has been emphasized recently because of its correlation with specific diseases such as dysfunction in the kidney and liver [137–141]. At normal physiological conditions, ammonia can be expelled from the slightly alkaline blood and emanated through the skin or exhaled with the breath. The detection of the ammonia present in breath or urine can be used for the early diagnosis

of liver or stomach diseases [138]. The development of sensing devices for measuring ammonia with a sensitivity of 50–2000 ppb and with a fast response time is highly desired [137].

To the best of our knowledge, there is still no OFS that is capable of measuring ammonia in the breath. Conventional methods for the ammonia measurements are mainly based on gas chromatography mass spectrometry, which, in spite of its high selectivity and sensitivity, is expensive, requires well trained operator and is time consuming. The development of cheap, small, sensitive and reliable sensor devices that can efficiently operate at different relative humidity (RH) levels can help to create a point-care medical system that can be used in daily life.

In past decades, a number of approaches to optical fibre based ammonia sensing utilizing sensitive coatings have been reported. Wolfbeis employed fluorescent measurements using optical fibre probe to measure pH of an indicator solution [142]. Since then, lossy mode resonances [143], EW [144–146] fibre gratings and reflection sensors at the tip of the fibre [147] have been reported. Generally, the LoD ranges from 10 to 100 s of ppm, which is too high for meaningful healthcare application. Table 4 summarizes some of the ammonia sensor parameters reported in the literature.

Although the detection of VOCs is not routinely conducted in clinical settings, it has high potential as a non-invasive diagnostic tool and much literature has been published on the relationship between diseases at the VOCs emitted from human body [150]. A sensor based on the cladding removed EW OFS modified with sensitive layer of dye compound that was tested on several humans was able to distinguish skin emanations from different people was reported in [151]. Using this sensor it was also possible to recognize changes in people's physiological conditions by applying a pattern recognition technique (principal component analysis) to analyse changes in the EW spectrum. The developed system has a significant advantage in size, simplicity of fabrication and cost as compared to the arrays of chemical sensors or more sophisticated gas chromatography techniques. Being able to

recognize qualitative changes in ‘global body odour’, the described system has the potential for further development for application in healthcare for disease diagnostics.

Several OFS have been used to detect VOCs, although none yet have sufficient sensitivity and selectivity for meaningful medical application [152]. There have been a number of fibre optic based VOC gas sensors proposed recently using the deposition of a sensitive layer on the fibre tip to form an FPI [153–157], or cladding removed EW sensors, where part of the cladding is mechanically or chemically removed and then the functional coating is deposited over the stripped region [158–162]. Coatings sensitive to VOC vapours have been also deposited onto the surface of photonic crystal fibres [163] and LPGs [164–166]. The reported sensors suffer mostly from a long response time, in the range of 10 s of minutes, and are usually tested over a limited but biologically relevant concentration range.

Humidity measurement plays an important role in the monitoring of air delivered to mechanically ventilated patients in critical care [167] and in monitoring the microenvironment of chronic wounds [168]. Humidification of inspired gases is an essential part of clinical treatment in critical respiratory care. Inhalation of inadequately humidified gas during invasive (through an ETT placed in the patient’s trachea) or non-invasive (via a mask placed on the patient’s face) ventilation, causes drying of the delicate respiratory mucosa and consequent cooling, mucosal injury, drying of (and difficulty in clearing) secretions and respiratory deterioration [169]. The clinically acceptable range of absolute humidity (AH) and RH values at the level of the upper trachea is between 5 mg l^{-1} (50% RH at 27°C – 28°C) and 42 mg l^{-1} (85% RH at 34°C nasal, 95% RH at 35°C naso/oropharynx) [170]. Requirements for response and recovery times of humidity sensors are driven by the respiration rate and typical need to be faster than 1 s [167].

A number of OFS configurations have been used to measure humidity, such as FPI using various humidity sensitive thin films [167, 171–175], de-clad plastic optical fibre [176, 177], hetero-core OFS [178] and microstructured optical fibres [179]. FBGs modified with materials that swell and contract when exposed to water can also be used to measure humidity [180], but this type of sensor possesses relatively slow response and recovery times and is thus not suitable for medical application.

The principle of operation of FPI humidity sensors is based on the detection of the RI change caused by the absorption of water molecules into a humidity sensitive film, which can provide fast response to changing humidity levels [167]. An FPI humidity sensor was reported recently that was tested within a mechanical ventilator to detect respiration rate, see figure 12 [167], and to determine the AH delivered into the lungs [181]. The response time was 1.5 s. The sensor has also been validated with animal models [100, 182].

Another application of humidity sensing is in wound healing [177]. A wound dressing that remotely monitors parameters associated with healing such as the humidity presented on the wound microenvironment, wound exudate pH and proliferative cell levels within the wound could have a significant impact on wound treatment. This monitoring would enable clinical interventions to take place promptly but only when required, thus improving wound care and reducing

the number of clinical appointments [183]. The humidity sensor had sensitivity of approximately -3.87×10^{-3} and -9.61×10^{-3} in transmittance percentage per RH percentage for the range of $\sim 10\%$ to $\sim 75\%$ RH and 90% to 97% RH, respectively. The proof of concept measurements made on the skin using a sensor embedded into a wound dressing, see figure 13, indicated that this sensor has the potential to be used to monitor the humidity of the skin microenvironment within a wound dressing, which can be used to provide better prognosis of healing.

4.1.2. Detection in liquid phase. Knowledge of the pH of human samples provides valuable information about diseases [184]. The pH in the human body can vary from 1.35 to 3.5 in the stomach to 8.0–8.8 in urine and pancreatic fluid. Table 5 provides a summary of the range of pH values and their function in the human body [184].

The pH level in serum has to be tightly controlled around to a value around 7.4 (a slightly alkaline range of 7.35–7.45) [185], which imposes strict demands on parameters of pH sensors, requiring a resolution better than 0.01 pH. The most popular approach to optical fibre based pH sensing relies on the use of dye indicators or fluorophores [186] deposited on tip of an optical fibre [187] or tapered optical fibres [17]. The principle of operation is based on detection of pH-induced colour change of the dye indicators, fluorescent intensity or the lifetime of fluorophores.

Recently, monitoring changes in polyelectrolytes deposited onto optical fibres has become an alternative approach for pH detection. The principle of operation is based on pH-induced swelling and contraction of the deposited film that results in a change of the optical thickness.

Shao *et al* [188] proposed an optical fibre pH sensor based on a TFBG coated with a pH sensitive polymeric film, poly (diallyldimethylammonium chloride) (PDDA) and poly (acrylic acid) (PAA), using the layer-by layer electrostatic self-assembly technique. A near-linear pH sensitivity of 117 arbitrary unit (a.u.)/pH unit and an accuracy of ± 1 a.u. (in the range of pH 4.66 to pH 6.02) with 10 s rise time and 18 s fall time for a sensor with six bilayers of PDDA/PAA was achieved. Gu *et al* [189] used a MI modified with poly (allylamine hydrochloride) and PAA nanocoatings to measure pH with the linear response in either acid or alkali solution (in the pH range 2.5–10) with resolution of 0.013 pH unit. Corers *et al* [190] coated polyelectrolyte structures onto an LPG for pH sensor development in the range of 4–7 pH units with sensitivity of 28.3 nm/pH and response recovery times of 120 s and 270 s, respectively. Goicoechea *et al* [191] used an FPI formed at the tip of an optical fibre using a coating of poly(allylamine hydrochloride) and the polymer PAA to detect pH with a resolution of 0.051 pH units.

Despite some of the reported optical fibre pH sensors being tested *in vivo* [192] and their commercial availability from Ocean Optics [193] and PreSens [194] with sufficient performance for medical applications, optical fibre pH sensor are yet to be routinely adopted in clinical settings. As noted by Mignani [44], this could be associated with some problems

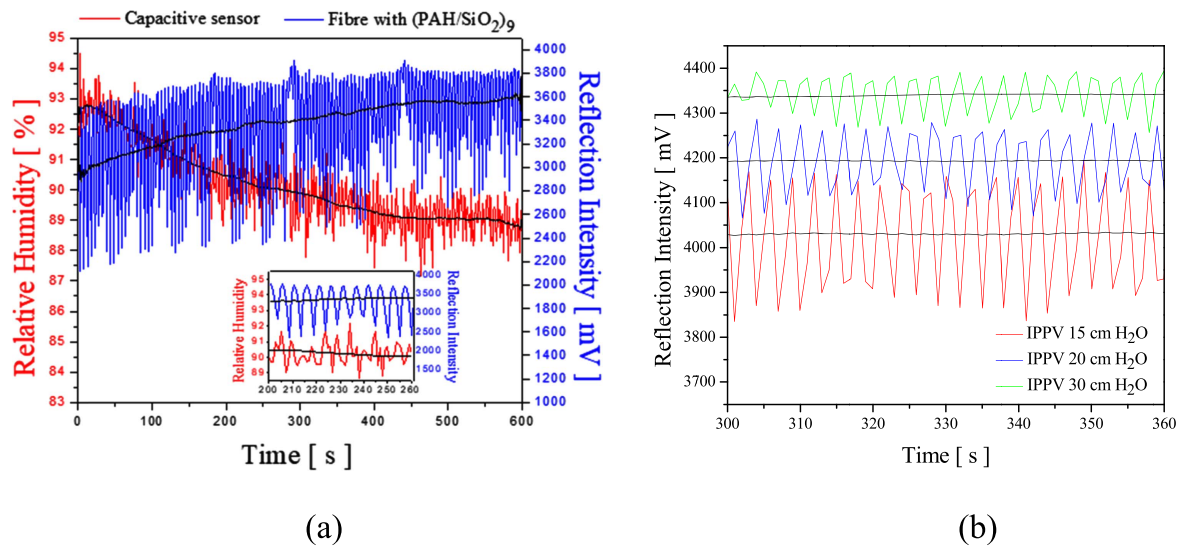


Figure 12. (a) Comparisons of OFS response (blue trace) and capacitive sensor response (red trace) at 15 cm H₂O in intermittent positive pressure ventilation (IPPV) mode and 12 breaths min⁻¹; the black traces correspond to the output of a moving average filter for each device response. During the measurement period, the temperature increased from 28.2 °C to 30.7 °C in the T-piece. The inset presents a zoom from 200 to 260 s of 15 cm H₂O in IPPV mode and 12 breaths min⁻¹; the optical fibre is the only sensor capable of measuring individual breaths due to its fast response; and (b) comparison of different pressures of IPPV for the same frequency of breaths min⁻¹; the behaviour shown is consistent for the whole experiment (600 s duration), the pressure of 15 cm H₂O always produced a higher RH than 20 cm H₂O and 30 cm H₂O. © 2016 IEEE. Reprinted, with permission, from [167].

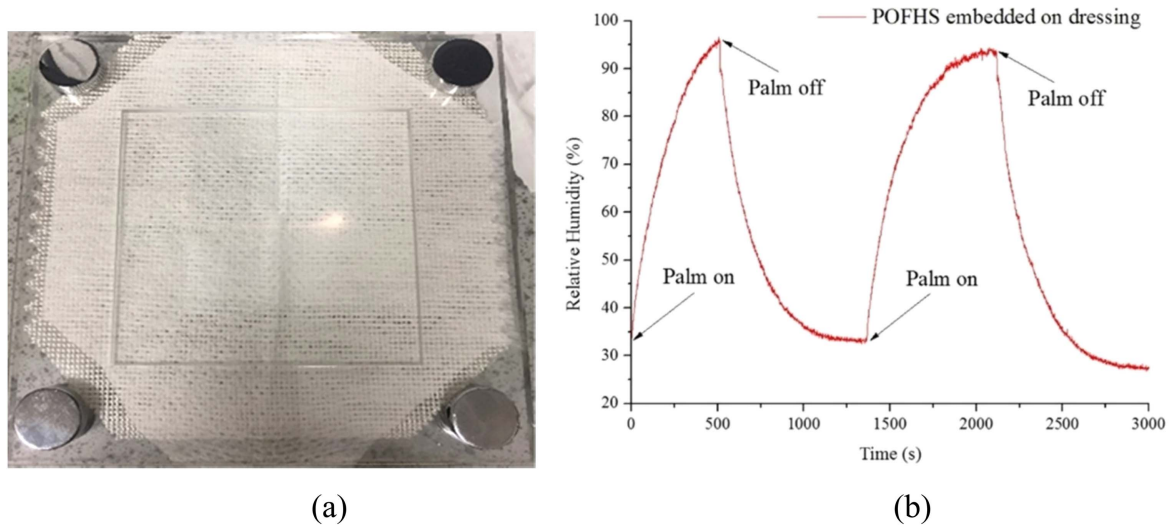


Figure 13. (a) POFHS embedded in a dressing and covered by a clinical gauze as a secondary dressing for humidity measurements. The unclad visible part of the sensor is 30 mm length. (b) *In vivo* humidity measurements on the palm of the hand recorded with the POFHS embedded on a dressing and covered with a clinical gauze as secondary dressing. Reprinted from [177], Copyright (2018), with permission from Elsevier.

that have emerged with the use of intravascular OFS, namely the formation of a thrombus around the sensor tip, which corrupts the measurement.

The detection of drug concentrations in biological fluids would aid the appropriate administration of pharmaceutical compounds to achieve efficient therapeutic effects in humans or animals [195]. Development of reliable sensors that can measure selectively a particular drug of interest with sufficient sensitivity and selectivity is an enormous task. Monitoring of the levels of antibiotics in the blood is an interesting area of

current OFS research, and successful development would open a possibility for personalized drug treatments allowing doses of medication to be given when the level in the blood drops to near the minimal effective dose. A vancomycin (VA) sensor based on an LPG modified with molecular imprinting polymers has been reported [196]. VA is a glycopeptide antibiotic derived from *Amycolatopsis Orientalis*. The mode of action of VA consists of the inhibition of cell wall biosynthesis and alteration of the permeability of the bacterial cell membrane. VA has been used to treat various serious

Table 5. pH of selected fluids, organs, and membranes reproduced from [184].

Organ, fluid or membrane	pH	Function of pH
Skin	Natural pH is between 4 and 6.5	Barrier protection from microbes
Urine	4.6 to 8.0	Limit overgrowth of microbes
Gastric	1.35 to 3.5	Break down protein
Bile	7.6 to 8.8	Neutralize stomach acid, aid in digestion
Pancreatic fluid	8.8	Neutralize stomach acid, aid in digestion
Vaginal fluid	<4.7	Limit overgrowth of opportunistic microbes
Cerebrospinal fluid	7.3	Bathes the exterior of the brain
Intracellular fluid	6.0–7.2	Due to acid production in cells
Serum venous	7.35	Tightly regulated
Serum arterial	7.4	Tightly regulated

gram-positive infections. It is a powerful antibiotic, which in high doses can be toxic to the ears and kidneys, whilst at low doses can cause hypersensitivity reactions. Thus it is important to measure accurately the concentration of VA in blood to control its administration to patients. Molecular imprinting is one of the most promising approaches for achieving specific molecular recognition. The technique is versatile, as any compound with functional groups can, in principle, be imprinted in different porogens (either water or organic solvents). The basic concept of molecular imprinting is based on the creation of imprints of the template compound (i.e. chemical molecules or biological species that needs to be detected—analytes) in a polymeric matrix, achieved by its incorporation during the polymerization step. The reported sensor was able to measure concentrations as low as 10 nM with high selectivity against other commonly prescribed antibiotics such as amoxicillin, bleomycin and gentamicin. In addition, the response of the sensor was characterized in a complex matrix, porcine plasma, spiked with 10 μM of VA. Adriamycin, an anthracycline antibiotic with antineoplastic activity, has also been detected using OFS [197]. Lu *et al* [197] proposed a fluorescence quenching sensor that was able to measure adriamycin with detection limits as low as 0.057 $\mu\text{g ml}^{-1}$ at a signal-to-noise ratio of 3. The developed sensor was tested *in vivo* on an animal model.

Propofol (2, 6-di-isopropylphenol) is an intravenous anaesthetic widely used during surgery and for continuous sedation in intensive care, and is another example of a drug where there is demand for its detection. Li *et al* [198] demonstrated a system for propofol detection using on-line molecularly imprinted polymer solid-phase extraction coupled to fluorescence optical fibre detection. The linearity was assessed from 0.10 to 15 mg ml^{-1} of propofol in whole blood.

4.2. Optical fibre Biosensors

The commonly accepted classical definition of a biosensor is [199]: ‘Biosensors are a particular class of devices, where the sensing unit is constituted by a biological recognition element, able to recognize in a highly specific manner a selected target or a class of compounds’. The key in this definition is ‘biological recognition element’ and therefore, as discussed

by Wang and Wolfbeis [200], ‘chemical sensors not using a biological component but placed in a biological matrix (such as a pH electrode in blood) are not biosensors by definition’. Recently, Socorro and Diaz [201] suggested that the biosensor definition should be updated and expanded to include ‘devices capable of monitoring a specific biomedical variable (including biochemical or physical) and provide information that can give a rapid and accurate diagnosis of a patient’s health condition’. Although this is an interesting suggestion, perhaps this definition is more suitable for a healthcare sensor rather than a biosensor and therefore in this review we will follow a classical definition of biosensor as a device with a biological recognition element. This biological recognition element, typically bound to an optical fibre via covalent bonding, could be an antibody [40, 202], an enzyme [203], a protein [204], or a nucleic acid [205] or even a whole cells [206, 207], chosen to recognize analytes via biochemical mechanisms.

The sensing system can be designed to operate in labelled and label-free mode. The former utilizes fluorescence labelling of the analyte and measures changes in fluorescence intensity caused by the interaction of analyte with the biological recognition element [202]. This approach is similar to enzyme-linked immunosorbent assay, ELISA, which is used routinely in healthcare [208]. In the development of optical fibre biosensors, there is more research effort devoted to the label-free mode, since it overcomes the disadvantages of the fluorescence methods, such as the additional labelling step and problems associated with fluorophores, for example their relatively short lifetime and photobleaching. The label-free approach is usually based on the detection of changes in optical thickness (product of RI and geometrical thickness) associated with the binding of analyte to the biological recognition element deposited onto an optical fibre. Optical fibre refractometers based on sensing platforms such as tapered optical fibres [209–213], LPGs [40, 214–220] and TFBG [221] coated with biological recognition elements have been explored for label-free bio-sensing.

Another interesting approach for label-free bio-sensing is based on so called plasmonic OFS [222]. This approach utilizes noble metals, typically gold or silver, (in the form of a film or nanoparticles) grafted with bioreceptors and deposited onto the surface of the optical fibre. The EW is used to excite

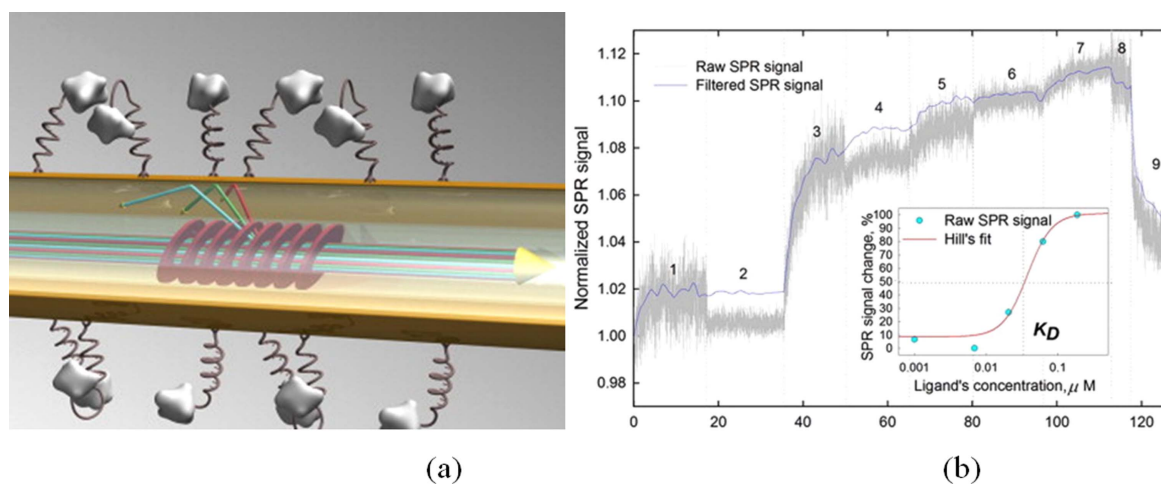


Figure 14. (a) Schematic diagram of gold coated tilted fibre Bragg grating surface plasmon resonance sensor coated with aptamer receptor molecules. (b) Normalized amplitude of the TFBG-SPR aptasensor as a function of time, for increasing concentrations of thrombin (the successive steps of the ladder are: (1) Milli-Q water; (2) DNA buffer; (3) aptamer, $20 \mu\text{M}$; (4) thrombin, $0.1 \mu\text{M}$; (5) thrombin, $0.5 \mu\text{M}$; (6) thrombin, $1 \mu\text{M}$; (7) thrombin, $5 \mu\text{M}$; (8) protein buffer; (9) regeneration in 0.2 M of Na_2CO_3). The inset in the figure illustrates the relationship between normalized SPR signal change and thrombin concentration, from which binding constant, K_D , can be estimated. Reprinted from [223], Copyright (2013), with permission from Elsevier.

plasmons (oscillation of electrons at the metal–dielectric interface), which are sensitive to the binding of analytes. One of the biggest advantages of plasmonic OFS over other label-free methods is their high sensitivity [223].

In healthcare, biosensors can be used to detect biomarkers or to detect bacteria directly. Albert *et al* [223] reported a plasmonic OFS based on a TFBG coated with a thrombin binding aptamer, figure 14(a), to detect the protein human α -thrombin, an important enzyme in the blood-clotting cascade, in its fibrinogen-binding exosite. The authors demonstrated that the specific interaction between the protein and the sensor lead to a signal increase after each new higher concentration, and that an increase of the SPR signal remained after a final protein buffer wash, revealing the binding of the analyte to the sensitive layer, figure 14(b).

The authors also proposed a concept for multiplexed TFBG-SPR sensors embedded across a microfluidic channel; figure 15 [223]. This concept allows application of several OFS in a multiplexed array, where the fibres were interrogated sequentially. Each sensor could have its surface functionalised with a different bio-receptor to capture different targets, to provide baseline reference data, or to improve the LOD through statistical analysis of the response of multiple identical sensors.

In a similar approach [205], an LPG was functionalised with an aptamer to detect the outer membrane proteins of *Escherichia coli* in the clinically relevant concentration range between 0.1 and 10 nM . The principle of operation is based on the measurement of the wavelength shift induced by the binding of the membrane protein. The sensor could be regenerated by treatment with acid. An example of an enzymatic optical fibre biosensor, where a particular enzyme is used to detect analyte, is a glucose sensor, which was reported in [224]. In glucose biosensors, glucose oxidase (GOx) is attached to the optical fibre and the change of RI due to the oxidation of glucose by GOx is measured. The sensor

operated in the $0\text{--}2.6 \text{ g l}^{-1}$ concentration range and was tested in whole blood.

Comprehensive reviews of optical fibre chemical and biosensors have been recently published [3, 199–201, 221]. There are no reports of optical fibre chemical or biosensors that have been used in clinical settings. Moreover, there are no publications that have validated optical fibre chemical and biosensors *in vivo*, with all published work stopping at the proof of concept stage in the laboratory setting. The possible reasons for this and also some suggestions how this can be overcome are discussed in the next section.

5. Adoption of OFS in healthcare

As described in this article, a wide range of mechanical and biochemical sensing configurations have been developed in the laboratory setting that have high potential to make a significant difference to healthcare. There have been some successes in niche applications [225] such as measurements of intracranial pressure (ICP by e.g. FISO, Canada) [86], intracuff air pressure in intra-aortic balloons (e.g. Arrow FiberOptix™ Technology by Teleflex, USA), temperature (e.g. Lumasense, USA) and blood pressure (Opsens Medical, Canada). These have been motivated by the advantages of OFS, including their small size, high performance and immunity from electromagnetic interference. However, it is reasonable to state that, aside from some successes in niche markets, optical fibre sensing has not fulfilled its promise in healthcare. This section offers observations by the authors on why this might be the case and suggests areas for consideration by those developing OFS in healthcare.

As described in section 2, the technology for pressure and temperature sensing [1, 2] is well established and although the costs of fibres and connectors are low they are still much higher than their wired equivalents. Furthermore,

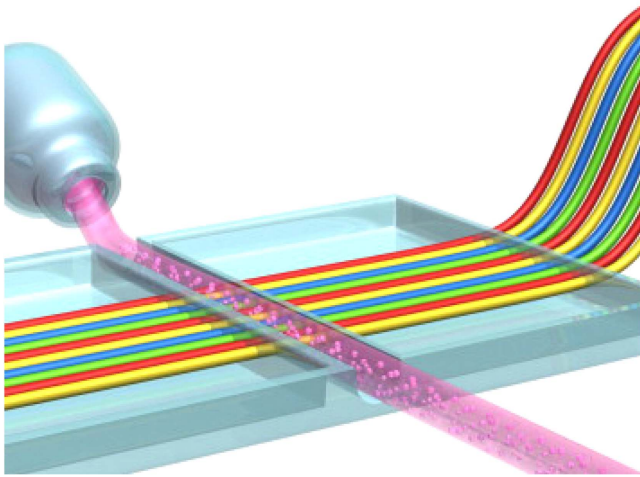


Figure 15. Artist conception of a multiplexed TFBG-SPR sensors embedded across a microfluidic channel. Reprinted from [223], Copyright (2013), with permission from Elsevier.

interrogation units utilizing tuneable lasers or spectrometers are expensive. Even though these can be used multiple times with disposable OFS, the field would benefit from lower cost interrogation units. Biochemical sensors are less well established in healthcare and research is still required in the development of robust, reproducible protocols that are acceptable for use within medical device regulations.

Bringing a medical device to market is a costly process due to the need to comply with medical device regulation and clinical studies. It is therefore important to understand *early in the development process* whether a device is likely to attract investment and eventually be adopted. Several papers have discussed the multiple factors associated with adoption of medical devices. Dymond *et al* [226] provide advice for bringing new medical technology to the marketplace. An innovative technology alone is insufficient and other drivers such as clinical need, competition with the state of the art and patient need are all identified as factors. Tasks such as market analysis; device design; research and development, prototyping, clinical trials, regulation and manufacturing can all be conducted in parallel. A case study reported in [227] discusses adoption of radiotherapy techniques and identifies a number of social (e.g. enthusiastic colleagues), financial (incentives) and scientific (clinical evidence) factors as being the main reasons that influenced adoption. Although addressing the specific case of technologies for healthy aging, Piau *et al* [228] pose useful questions that should be asked during device development and propose a framework for technology development that utilizes different evaluation approaches at different stages of the development process.

Although Rogers' diffusion of innovation theory [229] has relevance to healthcare there are some limitations when applied to public health. In common with diffusion of innovation, clinicians will be influenced by the utility of the innovation; any disruptions that it may cause to existing habits, personal or social values, social status of opinion

leaders and whether the clinician is an 'early adopter' or a 'laggard' [230]. Key clinical opinion leaders clearly have an important role but other stakeholders such as patients, health economists, government officials, managers, insurers and regulators are becoming increasingly important. However, diffusion of medical technology is different because [230]:

- (a) Health and illness is emotive and there is often a political commitment to offer citizens the latest advances.
- (b) New technologies promise better health and improved quality of life but are often associated with higher cost services. Due to scarce resources, decision makers have to prioritize.
- (c) There is a gap between 'best evidence' and 'evidence-based' practice and clinical evidence alone is insufficient to push forward the innovation.

A top-down approach of guidance, such as by the National Institute for Health and Care Excellence (NICE) in the UK aims to take an evidence-based approach to recommending medical devices and influences adoption decisions. The process for providing medical device guidance has been reviewed [231] and the main reasons for not recommending devices are lack of evidence, insufficient or uncertain benefit to the National Health Service (NHS), insufficient or uncertain benefit to patients, uncertain or no cost benefit, lack of novelty, lack of clarity as to how the technology would be used in NHS, wrong comparator, design appropriate only to a small population, usability or technology design issues, or the evidence does not translate to the UK setting and there is insufficient demand. It is also noted [232] that it is important to develop a good plausible value proposition to enable evaluation of the technology. Many smaller manufacturers do not properly understand how to construct a persuasive value proposition and the need to provide appropriate clinical evidence.

Much work has been conducted in developing models to assess and demonstrate the value of a new technology early in the development process (see Maarten *et al* [233] for a useful review). This approach has the potential to benefit developers of OFS technology by steering the area of application. A particularly useful framework for deciding whether to proceed with development of a new technology has been proposed [234], which includes competitor analysis, clinical application, value proposition and investor decision. Within this broader framework an early stage health economic assessment named the headroom method is proposed in which the new technology is compared with the current gold standard. The headroom method is based on optimistic but plausible assumptions about the performance of a new technology and then calculates the willingness to pay threshold of a device purchaser given this performance. If this amount is above the likely price of a device then a developer is likely to continue development, if this below then a developer should reconsider development or refine manufacturing strategy. It has also been

suggested [235] that this approach could be applied in academia where the research is applied or translational in nature.

Another key component of successful translation of medical devices into clinical use is to understand the needs of the end users. Devices need to be well designed to be safe, comply with regulations and also be usable. Better communication is required in order to ensure usable designs [236]. Focus groups are often used, but Martin *et al* [237] describe a range of ergonomics methods that are appropriate for eliciting the needs of end users at different stages in the development process. Many of these methods and the principles of ergonomics are accessible to device developers. A case study has also been provided to help demonstrate how a company was guided away from an application based on user engagement [237].

Additional hurdles are also the lack of standardized protocols capable of guaranteeing repeatable and reproducible results [3] and also, for *in vivo* applications, OFSs require initial calibration steps before any deployment inside the body, to overcome a different behaviour in complex matrix and a different uncalibrated response.

In summary, we believe that for those motivated in translating technologies into clinical practice, it is essential to understand the multi-factorial decisions made when adopting devices. Competing technologies and the clinical need has to be understood. Early stage health economic tools and engagement with end users should be performed early in the development process to guide the technology design and application area.

6. Conclusions and future directions

This paper reviews different types of OFS and their most recent applications in healthcare. It aims to help clinicians to understand OFS technology and to provide an overview of hurdles that OFS community faces during deployment of developed technology in healthcare.

As discussed, OFS offer great potential for healthcare applications. However, despite the maturity of the OFS technology and the advantages it offers, with few exceptions we can conclude that OFS technology has not realized its full potential in healthcare yet. We suggest that the following reasons are responsible for the low level of implementation of OFS in healthcare. Beware aware of, and addressing, these reasons will help to support widespread implementation of this promising technology.

A variety of types of OFS and inconsistency in reporting their performance make it difficult for end users (clinicians) to choose an appropriate design for optimal implementation in particular areas of healthcare. For instance, tapered optical fibres, despite their high sensitivity and simplicity in fabrication, require careful packaging as the mechanical strength of the fibre is reduced during tapering and it is not straightforward to use them *in vivo*.

There are a number of regulatory and adoption challenges of accepting technology in healthcare. For instance, there was a gap of 2.5 years between animal trials [100] and

the recently conducted human volunteer tests, of which 1 year was spent on completing regulatory documentation. Understanding early the value of a technology to healthcare providers is very important in the device development process.

There has however been successful testing of OFS *in vivo*, measuring temperature, pressure and strain using grating based approaches. Sensors based on gratings retain the mechanical stability of the optical fibre and also avoid referencing issues. It is also worth noting that these examples are comprised of physical parameters as these are generally easier to detect and use in diagnostics than biochemical measurands. We believe that the most promising future directions are in niche applications of OFS technology, where no other sensors can be deployed, and also in systems capable of multi-parameter measurements, where a single optical fibre with a number of multiplexed sensors provides information simultaneously on several variables. Again, understanding user requirements is important early in the development process.

For chemical and biosensors it is noted that the use of OFS technology to detect gases emitted from human body is fairly mature in research terms and there are many such sensors reported, but again with limited examples of *in vivo* applications. There are no examples of *in vivo* applications of biosensors. Which most likely is owing to the complexity of sensor development, which needs to take into account not only the design of the OFS but also that of the sensitive layer deposited onto the optical fibre. It also requires pre-calibration steps to take into account complex medium for *in vivo* applications. In the majority of cases, the response of these sensors is non-reversible and their lifetime is limited by the lifetime of the sensitive layer, which makes it difficult in practical implementation and additional steps of sample collection are required. Future directions will evolve in the development of robust OFS that can be tested *in vivo*. For instance, these sensors could use grating based biosensors modified with artificial bioreceptors, such as molecularly imprinted polymers, as they are more stable than natural enzyme/DNA/aptamer based bioreceptors. For *in vitro* applications in analytical sciences, OFS can be used to measure minute volumes (in order of femtolitres [238]) of human samples, which is especially attractive when volume these samples is limited, for instance saliva, tears and inner-ear fluids.

Acknowledgments

This work was supported by the Engineering and Physical Sciences Research Council (Grant Nos. EP/N026985/1, EP/N025725/1).

ORCID iDs

S James  <https://orcid.org/0000-0003-0651-9842>

S-W Lee  <https://orcid.org/0000-0001-7329-065X>

S P Morgan  <https://orcid.org/0000-0003-4069-3801>

S Korposh  <https://orcid.org/0000-0001-5179-6991>

References

- [1] Poeggel S, Tosi D, Duraibabu D B, Leen G, McGrath D and Lewis E 2015 Optical fibre pressure sensors in medical applications *Sensors* **15** 17115–48
- [2] Schena E *et al* 2016 Fiber optic sensors for temperature monitoring during thermal treatments: an overview *Sensors* **16** 1144
- [3] Chiavaioli F *et al* 2017 Towards a uniform metrological assessment of grating-based optical fiber sensors: from refractometers to biosensors *Biosensors* **7** 23
- [4] Hecht J 1999 *City of Light, The Story of Fiber Optics* (New York: Oxford University Press) p 114
- [5] Tyndall J 1869 *Notes of a Course of Nine Lectures on Light delivered at the Royal institution of Great Britain* 8 April–3 June (London: Longmans)
- [6] Parries M C 1989 Optical fibre *Contemp. Phys.* **30** 303–4
- [7] <https://thorlabs.com/catalogPages/1100.pdf> (Accessed: 17 January 2018)
- [8] https://thorlabs.com/newgrouppage9.cfm?objectgroup_ID=7840 (Accessed: 17 January 2018)
- [9] https://thorlabs.com/newgrouppage9.cfm?objectgroup_id=6838 (Accessed: 10 January 2018.)
- [10] Grattan K and Meggitt B 1999 *Chemical and Environmental Sensing* (Boston, MA: Kluwer Academic)
- [11] Mehvar M, BIS C, Scharer C M, Young M M and Luong J H 2000 Fiber-optic biosensors-trends and advances *Anal. Sci.* **16** 677–672
- [12] Seitz W R 1984 Chemical sensors based on fibre optics *Anal. Chem.* **56** 16–34
- [13] Korposh S, Kodaira S, Lee S-W, Batty W J and James S W 2009 Nano-assembled thin film gas sensor: II. An intrinsic high sensitive fibre optic sensor for ammonia detection *Sensor Mater.* **21** 179–89
- [14] Fang Y-L, Wang C-T and Chiang C-C 2016 A small U-shaped bending-induced interference optical fiber sensor for the measurement of glucose solutions *Sensors* **16** 1460
- [15] Lucas P, Coleman G J, Jiang S, Luo T and Yang Z 2015 Chalcogenide glass fibers: optical window tailoring and suitability for bio-chemical sensing *Opt. Mater.* **47** 530–6
- [16] Jarzebinska R, Korposh S, James S, Batty W, Tatam R and Lee S-W 2012 Optical gas sensor fabrication based on porphyrin-anchored electrostatic self-assembly onto tapered optical fibres *Anal. Lett.* **45** 1297–309
- [17] Jarzebinska R, Cheung C S, James S W and Tatam R P 2009 Response of the transmission spectrum of tapered optical fibres to the deposition of a nanostructured coating *Meas. Sci. Technol.* **20** 034001
- [18] Stewart W J and Love J D 1985 Design limitations on tapers and couplers in single mode fibres *Technical Digest, 5th Int. Conf. on Integrated Optics and Optical Fiber Communication-11th European Conf. on Optical Communication* (Venice)
- [19] Latif H, Zibaii M, Hossein S M and Jorge P 2012 Nonadiabatic tapered optical fiber for biosensor applications *Photonic Sensors* **2** 340–56
- [20] Mackenzie H S and Payne F P 1990 Evanescent field amplification in a tapered single-mode optical fibre *Electron. Lett.* **26** 130–2
- [21] Massaro A, Pierantoni L and Rozzi T 2006 Far-field radiation of optical fibres with tapered end *J. Lightwave Technol.* **24** 3162–8
- [22] Love J D, Henry W M, Stewart W J, Black R J, Lacroix S and Gonthier F 1991 Tapered single-mode fibres and devices: I. Adiabaticity criteria *IEE Proc. J.—Optoelectron.* **138** 343–54
- [23] Vahala K J 2003 Optical microcavities *Nature* **424** 839–46
- [24] Edwards P S, Janisch C T, He L, Zhu J, Yang L and Liu Z 2012 Fibre taper based Raman spectroscopic sensing *Photonics Conf. (IPC)* (IEEE) pp 501–2
- [25] Brambilla G 2010 Optical fibre nanotaper sensors *Opt. Fibre Technol.* **16** 331–42
- [26] Brambilla G 2010 Optical fibre nanowires and microwires: a review *J. Opt.* **12** 043001
- [27] Farnesi D *et al* 2015 Quasi-distributed and wavelength selective addressing of optical micro-resonators based on long period fiber gratings *Opt. Express* **23** 21175–80
- [28] Maite I *et al* 2017 Tapered optical fiber sensor for chemical pollutants detection in seawater *Meas. Sci. Technol.* **28** 045802
- [29] Lee B H, Kim Y H, Park K S, Eom J B, Kim M J, Rho B S and Choi H Y 2012 Interferometric fiber optic sensors *Sensors* **12** 2467–86
- [30] Corres J M, Matias I R, Bravo J and Arregui F G 2008 Tapered optical fibre biosensor for the detection of anti-gliadin antibodies *Sensors Actuators B* **135** 608–11
- [31] Kashyap R 2010 *Fiber Bragg Gratings* (San Diego, CA: Academic)
- [32] Massaroni C, Caponero M A, D'Amato R, Lo Presti D and Schena E 2017 Fiber Bragg grating measuring system for simultaneous monitoring of temperature and humidity in mechanical ventilator *Sensors* **17** S17040749
- [33] Maguis S *et al* 2008 Biofunctionalized tilted fiber Bragg gratings for label-free immunosensing *Opt. Express* **16** 19049–62
- [34] James S W and Tatam R P 2003 Optical fibre long-period grating sensors: characteristics and application *Meas. Sci. Technol.* **14** R49–61
- [35] Korposh S, Lee S-W and James S 2017 Long period grating based fibre optic chemical sensors *Fiber Optic Sensors: Current Status and Future Possibilities* ed I R Matias *et al* (Bern: Springer) pp 241–67
- [36] Bhatia V 1999 Applications of long-period gratings to single and multi-parameter sensing *Opt. Express* **4** 457–66
- [37] Bhatia V, Campbell D K, Sherr D, Dalberto T G, Zabaronick N A, TenEyck G A, Murphy K A and Claus R O 1997 Temperature-insensitive and strain-insensitive long-period grating sensors for smart structures *Opt. Eng., Bellingham* **36** 1872–6
- [38] Korposh S, James S W, Lee S-W, Topliss S, Cheung S C, Batty W J and Tatam R P 2010 Fiber optic long period grating sensors with a nanoassembled mesoporous film of SiO₂ nanoparticles *Opt. Express* **18** 13227–38
- [39] Wong R Y, Chehura E, Staines S E, James S W and Tatam R P 2014 Fabrication of fiber optic long period gratings operating at the phase matching turning point using an ultraviolet laser *Appl. Opt.* **53** 4669–74
- [40] Marques L, Hernandez F U, James S W, Morgan S P, Clark M, Tatam R P and Korposh S 2016 Highly sensitive optical fibre long period gratings biosensor anchored with silica core gold shell nanoparticles *Biosens. Bioelectron.* **75** 222–31
- [41] Cheung S C, Topliss S M, James S W and Tatam R P 2008 Response of fibre optic long period gratings operating near the phase matching turning point to the deposition of nanostructured coatings *J. Opt. Soc. Am. B* **25** 897–902
- [42] Stavem K, Saxholm H and Smith-Erichsen N 1997 Accuracy of infrared ear thermometry in adult patients *Intensive Care Med.* **23** 100–5
- [43] Teunissen L P J *et al* 2011 Limitations of temperature measurement in the aural canal with an ear mould integrated sensor *Physiol. Meas.* **32** 1403
- [44] Mignani A G and Baldini F 1996 Biomedical sensors using optical fibres *Rep. Prog. Phys.* **59** 1–28

- [45] Lewis E, Staruch M A and Chopra R 2015 Thermometry and ablation monitoring with ultrasound *Int. J. Hyperth.* **31** 163–81
- [46] Christensen D A 1988 Fiberoptic temperature sensing for biomedical applications *Proc. SPIE* **906** 108–13
- [47] Dziuda L, Krej M and Skibniewski F W 2013 Fiber Bragg grating strain sensor incorporated to monitor patient vital signs during MRI *IEEE Sens. J.* **13** 4986–91
- [48] Su H *et al* 2017 Fiber-optic force sensors for MRI-guided interventions and rehabilitation: a review *IEEE Sens. J.* **17** 1952–63
- [49] LumaSense Technologies <http://lumasenseinccom/> (Accessed: 17 January 2017)
- [50] Grattan K T V and Zhang Z Y 1995 *Fiber Optic Fluorescence Thermometry* (Berlin: Springer)
- [51] Zhang Z, Grattan K and Palmer A W 1992 A Fiber-optic high-temperature sensor based on the fluorescence lifetime of alexandrite *Rev. Sci. Instrum.* **63** 3869
- [52] Berthou H and Jörgensen C K 1990 Optical-fiber temperature sensor based on upconversion-excited fluorescence *Opt. Lett.* **15** 1100–2
- [53] Froggatt M E, Gifford D K, Kreger S, Wolfe M and Soller B J 2006 Characterization of polarization-maintaining fiber using high-sensitivity optical-frequency-domain reflectometry *J. Lightwave Technol.* **24** 4149–54
- [54] Tosi D, Macchi E and Cigada A 2015 Fiber-optic temperature and pressure sensors applied to radiofrequency thermal ablation in liver phantom: methodology and experimental measurements *J. Sens.* **2015** 909012
- [55] Tosi D, Macchi E, Braschi G and Gallati M 2014 Monitoring of radiofrequency thermal ablation in liver tissue through fibre Bragg grating sensors array *Electron. Lett.* **50** 981–3
- [56] Rao Y J, Webb D J, Jackson D A, Zhang L and Bennion I 1997 In-fiber bragg-grating temperature sensor system for medical applications *J. Lightwave Technol.* **15** 779–84
- [57] Wolthuis R A, Mitchell G L, Hartl J C and Fromowitz M A 1991 Development of medical pressure and temperature sensors employing optical spectrum modulation *IEEE Trans. Biomed. Eng.* **38** 974–81
- [58] Kist R, Drope S and Wolfelschneider H 1984 Fiber-Fabry–Perot (FFP) thermometer for medical applications *Proc. 2nd Int. Conf. on Optical Fiber Sensors (OFS '84)* ed R Th Kersten and R Kist (Berlin: VDE) pp 165–70
- [59] Wu J L and Wang Y T 2006 A fluorescence optic-fiber temperature sensor using phase-locked detection with pulse modulation single reference *J. Phys.: Conf. Ser.* **48** 101
- [60] Polito D, Caponero M A, Polimadei A, Saccomandi P, Massaroni C, Silvestri S and Schena E 2015 A needle-like probe for temperature monitoring during laser ablation based on FBG: manufacturing and characterization *J. Med. Device* **2015** 9
- [61] Morris P, Hurrell A, Shaw A, Zhang E and Beard P A 2009 Fabry–Perot fiber-optic ultrasonic hydrophone for the simultaneous measurement of temperature and acoustic pressure *J. Acoust. Soc. Am.* **125** 3611–22
- [62] Macchi E G, Tosi D, Braschi G, Gallati M, Cigada A, Busca G and Lewis E 2014 Optical fiber sensors-based temperature distribution measurement in *ex vivo* radiofrequency ablation with submillimeter resolution *J. Biomed. Opt.* **19** 117004
- [63] Gifford D K *et al* 2005 Distributed fiber-optic temperature sensing using Rayleigh backscatter *ECOC Proc.* vol 3, pp 511–2
- [64] Mishra V, Singh N, Tiwari U and Kapur P 2011 Fiber grating sensors in medicine: current and emerging applications *Sensors Actuators A* **167** 279–90
- [65] Poeggel S *et al* 2015 Recent improvement of medical optical fibre pressure and temperature sensors *Biosensors* **5** 432–49
- [66] Fajkus M, Nedoma J, Martinek R, Vasinek V, Nazeran H and Siska P A 2017 Non-invasive multichannel hybrid fiber-optic sensor system for vital sign monitoring *Sensors* **17** 111
- [67] Samset E, Mala T, Edwin B, Gladhaug I, Søreide O and Fosse E 2001 Validation of estimated 3D temperature maps during hepatic cryo surgery *Magn. Reson. Imaging* **19** 715–21
- [68] Yoo W-J, Jang K-W, Seo J-K, Heo J-Y, Moon J-S, Park J-Y and Lee B-S 2010 Development of respiration sensors using plastic optical fiber for respiratory monitoring inside MRI System *J. Opt. Soc. Korea* **14** 235–9
- [69] Musolino S, Scharfner E P, Tsiminis G, Salem A, Monro T M and Hutchinson M R 2016 Portable optical fiber probe for *in vivo* brain temperature measurements *Biomed. Opt. Express* **7** 3069–77
- [70] Wei T, Han Y, Li Y, Tsai H-L and Xiao H 2008 Temperature-insensitive miniaturized fiber inline Fabry–Perot interferometer for highly sensitive refractive index measurement *Opt. Express* **16** 5764–9
- [71] Dobb H, Kalli K and Webb D J 2004 Temperature-insensitive long period grating sensors in photonic crystal fibre *Electron. Lett.* **40** 657–8
- [72] Hromadka J, Korposh S, Partridge M C, James S W, Davis F, Crump D and Tatam R P 2017 Multi-parameter measurements using optical fibre long period gratings for indoor air quality monitoring *Sensors Actuators B* **244** 217–25
- [73] Clausen I and Glott T 2014 Development of clinically relevant implantable pressure sensors: perspectives and challenges *Sensor* **14** 17686
- [74] Morrell K C, Hodge W A, Krebs D E and Mann R W 2005 Corroboration of *in vivo* cartilage pressures with implications for synovial joint tribology and osteoarthritis causation *Proc. Natl Acad. Sci. USA* **102** 14819–24
- [75] ANSI/AAMI 1994 Blood pressure transducers *Technical Report ANSI/AAMI BP22 AAMI*: Arlington, VA, USA
- [76] Pleros N, Kanellos G T and Papaioannou G 2009 Optical fiber sensors in orthopedic biomechanics and rehabilitation *9th Int. Conf. on Information Technology and Applications in Biomedicine (Larnaca)* pp 1–4
- [77] Al-Fakih E, Osman N A A and Adikan F R M 2012 The use of fiber Bragg grating sensors in biomechanics and rehabilitation applications: the state-of-the-art and ongoing research topics *Sensors* **12** 12890–926
- [78] Kanellos G T, Papaioannou G, Tsiokos D, Mitrogiannis C, Nianios G and Pleros N 2010 Two dimensional polymer-embedded quasi-distributed FBG pressure sensor for biomedical applications *Opt. Express* **18** 179–86
- [79] Ahmad H, Chong W Y, Thambiratnam K, Zulkifli M Z, Poopalan P, Thant M M M and Harun S W 2009 High sensitivity fiber Bragg grating pressure sensor using thin metal diaphragm *IEEE Sens. J.* **9** 1654–9
- [80] Arkwright J W, Underhill I D, Maunder S A, Blenman N, Szczesniak M M, Wiklendt L, Cook I J, Lubowski D Z and Dinning P G 2009 Design of a high-sensor count fibre optic manometry catheter for *in vivo* colonic diagnostics *Opt. Express* **17** 22423–31
- [81] Islam M R, Ali M M, Lai M H, Lim K S and Ahmad H 2014 Chronology of Fabry–Perot interferometer fiber-optic sensors and their applications: a review *Sensors* **14** 7451–88
- [82] Roriz P *et al* 2012 Fiber optic intensity-modulated sensors: a review in biomechanics *Photonic Sensors* 2012 **2** 315–30
- [83] Clark F, Schmidt E and DeLaCroix R 1965 Fiber optic blood pressure catheter with frequency response from DC into the audio range *Proc. National Electronics Conf. (McCormick Place, Chicago, IL, 25–27 October)* pp 213–6
- [84] Lekholm A and Lindström L H 1969 Optoelectronic transducer for intravascular measurements of pressure variations *Med. Biol. Eng. Comput.* **7** 333–5

- [85] Müller J H, Scheffer C and Elvin A 2008 *In vivo* detection of patellar tendon creep using a fiber-optic sensor *Int. J. Med. Eng. Inform.* **1** 155–73
- [86] Pinet É 2011 Pressure measurement with fiber-optic sensors: commercial technologies and applications *Proc. SPIE* **7753** 775304
- [87] Xu M G, Reekie L, Chow Y T and Dakin J P 1993 Optical in-fibre grating high pressure sensor *Electron. Lett.* **29** 398–9
- [88] Correia R R *et al* 2007 A pressure sensor based upon the transverse loading of a sub-section of an optical fibre Bragg grating *Meas. Sci. Technol.* **18** 3103
- [89] Correia R, Blackman O R, Hernandez F U, Korposh S, Morgan S P, Hayes-Gill B R, James S W, Evans D and Norris A 2016 Highly sensitive contact pressure measurements using FBG patch in endotracheal tube cuff *Proc. SPIE* **9916** 99161F
- [90] (<http://fisocom/sectionphp?p=17>) (Accessed: 21 December 2017)
- [91] Roriz P, Frazão O, Lobo-Ribeiro A B, Santos J L and Simões J A 2013 Review of fiber-optic pressure sensors for biomedical and biomechanical applications *J. Biomed. Opt.* **18** 50903
- [92] Dennison C R and Wild P M 2008 Enhanced sensitivity of an in-fibre Bragg grating pressure sensor achieved through fibre diameter reduction *Meas. Sci. Technol.* **19** 1–11
- [93] Kaufman K R *et al* 2013 Performance characteristics of a pressure microsensor *J. Biomech.* **36** 283–7
- [94] Cottler P *et al* 2009 Performance characteristics of a new generation pressure microsensor for physiologic applications *Ann. Biomed. Eng.* **37** 1638–45
- [95] OPSENS Fiber optic miniature pressure sensor (<http://opsens.com/en/industries/products/pressure/opp-m/>) (Accessed: 10 January 2017)
- [96] Cibula E and Donlagic D 2005 Miniature fiber-optic pressure sensor with a polymer diaphragm *Appl. Opt.* **44** 2736–44
- [97] Lindström L H 1970 Miniaturized pressure transducer intended for intravascular use *IEEE Trans. Bio-Med. Eng.* **17** 207–19
- [98] Black J M, Cuddigan J E, Walko M A, Didier L A, Lander M J and Kelpel M R 2010 Medical device related pressure ulcers in hospitalized patients *Int. Wound J.* **7** 358–65
- [99] Medical Devices and Vulnerable Skin Network Annual Report 2014–15 www.southampton.ac.uk/mdvsn (Accessed: 17 January 2017)
- [100] Correia R, Sinha R, Norris A, Korposh S, Talbot S, Hernandez F U, Hayes-Gill B R and Morgan S P 2017 Optical fibre sensing at the interface between tissue and medical device *Proc. SPIE* **10340** 103400X
- [101] Parkinson L A, van Zanten M, Piller N and Arkwright J W 2017 A high-resolution tape sensor improves the accuracy of applied pressure profiles during lower-leg bandaging—results from a study using a fibre-optic sensing tape *Int. Wound J.* **14** 973–7
- [102] Hsiao-Chuan Wang D, Blenman N, Maunder S, Patton V and Arkwright J 2013 An optical fiber Bragg grating force sensor for monitoring sub-bandage pressure during compression therapy *Opt. Express* **21** 19799–807
- [103] Dziuda L *et al* 2012 Monitoring respiration and cardiac activity using fiber Bragg grating-based sensor *IEEE Trans. Biomed. Eng.* **59** 1934–42
- [104] Jia D *et al* 2017 A fiber Bragg grating sensor for radial artery pulse waveform measurement *IEEE Trans. Biomed. Eng.* **65** 839–46
- [105] Sharath U *et al* 2013 Blood pressure evaluation using sphygmomanometry assisted by arterial pulse waveform detection by fiber Bragg grating pulse device *J. Biomed. Opt.* **18** 067010
- [106] Leitão C *et al* 2015 Central arterial pulse waveform acquisition with a portable pen-like optical fiber sensor *Blood Press. Monit.* **20** 43–6
- [107] Allsop T D P *et al* 2003 Embedded progressive-three-layered fiber long-period gratings for respiratory monitoring *J. Biomed. Opt.* **8** 552–8
- [108] Allsop T D P, Carroll K, Lloyd G, Webb D J, Miller M and Bennion I 2007 Application of long-period-grating sensors to respiratory plethysmography *J. Biomed. Opt.* **12** 064003
- [109] D'Angelo L T *et al* 2008 A system for respiratory motion detection using optical fibers embedded into textile *30th Annual Int. Conf. of the IEEE Engineering in Medicine and Biology Society (IEEE)* (<https://doi.org/10.1109/IEMBS.2008.4650011>)
- [110] Zheng Y L *et al* 2014 Unobtrusive sensing and wearable devices for health informatics *IEEE Trans. Biomed. Eng.* **61** 1538–54
- [111] Dziuda L 2015 Fiber-optic sensors for monitoring patient physiological parameters: a review of applicable technologies and relevance to use during magnetic resonance imaging procedures *J. Biomed. Opt.* **20** 010901
- [112] Charkoudian N 2003 Skin blood flow in adult human thermoregulation: how it works, when it does not, and why *Mayo Clin. Proc.* **78** 603–12
- [113] Jafarzadeh H 2009 Laser doppler flowmetry in endodontics: a review *Int. Endodontic J.* **42** 476–90
- [114] Charrett T O H, James S W and Tatam R P 2013 Optical fibre laser velocimetry: a review *Meas. Sci. Technol.* **23** 032001
- [115] MacDonald S, Michel K, LeCoq D, Boussard-Plédel C and Bureau B 2004 Optical analysis of infrared spectra recorded with tapered chalcogenide glass fibers *Opt. Mater.* **25** 171–8
- [116] Trolès J and Brilland L 2017 Chalcogenide microstructured optical fibres for mid-IR applications *C. R. Phys.* **18** 19–23
- [117] Sanghera J, Kung F, Pureza P, Nguyen V and Miklos Aggarwal I 1994 Infrared evanescent-absorption spectroscopy with chalcogenide glass fiber *Appl. Opt.* **33** 6315–632
- [118] Anne M-L *et al* 2009 Chalcogenide glass optical waveguides for infrared biosensing *Sensors* **9** 7398
- [119] Wiercigroch E *et al* 2017 Raman and infrared spectroscopy of carbohydrates: a review *Spectrochim. Acta A* **185** 317–35
- [120] Wilhelm A, Lucas P, DeRosa D and Riley M 2007 Biocompatibility of Te–As–Se glass fibers for cell-based bio-optic infrared sensors *J. Mater. Res.* **22** 1098–104
- [121] Korposh S, James S, Tatam R and Lee S-W 2013 Fibre-optic chemical sensor approaches based on nanoassembled thin films: a challenge to future sensor technology *Optical Fiber ed S W Harun (Rijeka: InTech) ch 9* (<https://doi.org/10.5772/53399>)
- [122] Ohira S I and Toda K 2008 Micro gas analyzers for environmental and medical applications *Anal. Chim. Acta* **619** 143–56
- [123] Turner A P F and Magan N 2004 Electronic noses and disease diagnostics *Nat. Rev. Microbiol.* **2** 160–6
- [124] Pavlou A K, Magan N, Jones J M, Brown J, Klatser P and Turner A P F 2004 Detection of *Mycobacterium tuberculosis* (TB) *in vitro* and *in situ* using an electronic nose in combination with a neural network system *Biosens. Bioelectron.* **20** 538–44
- [125] Kodogiannis V and Wadge E 2005 The use of gas-sensor arrays to diagnose urinary tract infections *Int. J. Neural Syst.* **15** 363–76
- [126] Dalton P, Gelperin A and Preti G 2004 Volatile metabolic monitoring of glycemic status in diabetes using electronic olfaction *Diabetes Technol.* **6** 534–44
- [127] Voss A, Baier V, Reisch R, von Roda K, Elsner P, Ahlers H and Stein G 2005 Smelling renal dysfunction via electronic nose *Ann. Biomed. Eng.* **33** 656–60

- [128] Haick H, Hakim M, Patrascua M, Levenberg C, Shehada N, Nakhoul F and Abassi Z 2009 Sniffing chronic renal failure in rat models via an array of random network of single-walled carbon nanotubes *ACS Nano* **3** 1258–66
- [129] Peng G *et al* 2009 Diagnosing lung cancer in exhaled breath using gold nanoparticles *Nat. Nanotechnol.* **4** 669–73
- [130] Ohira S I, Li J, Lonneman W A, Dasgupta P K and Toda K 2007 Can breath isoprene be measured by ozone chemiluminescence? *Anal. Chem.* **79** 2641–9
- [131] Righettoni M, Tricoli A and Pratsinis S E 2010 Si:WO₃ sensors for highly selective detection of acetone for easy diagnosis of diabetes by breath analysis *Anal. Chem.* **82** 3581–7
- [132] Toda K, Li J and Dasgupta P K 2006 Measurement of ammonia in human breath with a liquid-film conductivity sensor *Anal. Chem.* **78** 7284–91
- [133] Ding M and Brambilla G 2015 Optical fibres and sensors for biomedical applications *Biophotonics for Medical Applications (Woodhead Publishing Series in Biomaterials)* ed I Meglinski (Cambridge: Woodhead) ch 3 pp 53–78
- [134] Wolfbeis O S, Weis L J, Leiner M J P and Ziegler W E 1988 Fiber-optic fluorosensor for oxygen and carbon dioxide *Anal. Chem.* **60** 2028–30
- [135] Kolle C, Gruber W, Trettnak W, Biebernik K, Dolezal C, Reiningner F and O'Leary P 1997 Fast optochemical sensor for continuous monitoring of oxygen in breath-gas analysis *Sensors Actuators B* **38** 141–9
- [136] Hromadka J, Tokay B, Correia R, Morgan S P and Korposh S 2018 Carbon dioxide measurements using long period grating optical fibre sensor coated with metal organic framework HKUST-1 *Sensors Actuators B* **255** 2483–94
- [137] Timmer B, Olthuis W and Van den Berg A 2005 Ammonia sensors and their applications—a review *Sensors Actuators B* **107** 666–77
- [138] Turner C, Španěl P and Smith D 2006 A longitudinal study of ammonia, acetone and propanol in the exhaled breath of 30 subjects using selected ion flow tube mass spectrometry, SIFT-MS *Physiol. Meas.* **27** 321–37
- [139] Weiner I D, Mitch W E and Sands J M 2014 Urea and ammonia metabolism and the control of renal nitrogen excretion *Clin. J. Am. Soc. Nephrol.* **10** 1444–58
- [140] Schmidt F M, Vaittinen O, Metsälä M, Lehto M, Forsblom C, Groop P H and Halonen L 2013 Ammonia in breath and emitted from skin *J. Breath Res.* **7** 017109
- [141] Narasimhan L R, Goodman W and Patel C K N 2001 Correlation of breath ammonia with blood urea nitrogen and creatinine during hemodialysis *Proc. Natl Acad. Sci. USA* **98** 4617–21
- [142] Wolfbeis O S and Posch H E 1986 Fibre-optic fluorescing sensor for ammonia *Anal. Chim. Acta* **185** 321–7
- [143] Tiwari D, Mullaney K, Korposh S, James S W, Lee S-W and Tatam R P 2017 An ammonia sensor based on Lossy mode resonances on a tapered optical fibre coated with porphyrin-incorporated titanium dioxide *Sensors Actuators B* **242** 645–52
- [144] Rodríguez A J *et al* 2014 A fiber optic ammonia sensor using a universal pH indicator *Sensors* **143** 4060–73
- [145] Yagi T *et al* 1997 Fiber-optic ammonia sensors utilizing rectangular-cladding eccentric-core fiber *Opt. Rev.* **4** 596–600
- [146] Cao W and Duan Y 2005 Optical fiber-based evanescent ammonia sensor *Sensors Actuators B* **110** 252–9
- [147] Wang T, Yasukochi W, Korposh S, James S W, Tatam R P and Lee S-W 2016 A long period grating optical fiber sensor with nano-assembled porphyrin layers for detecting ammonia gas *Sensors Actuators B* **228** 573–80
- [148] Galbarra D *et al* 2005 Ammonia optical fiber sensor based on self-assembled zirconia thin films *Smart Mater. Struct.* **14** 739–44
- [149] Chu C-S and Chen Y-F 2017 Development of ratiometric optical fiber sensor for ammonia gas detection *Proc. SPIE* **10323** 103231P
- [150] Shirasu M and Touhara K 2011 The scent of disease: volatile organic compounds of the human body related to disease and disorder *J. Biochem.* **150** 257–66
- [151] Selyanchyn R, Korposh S, Yasukochi W and Lee S-W 2011 A preliminary test for skin gas assessment using a porphyrin based evanescent wave optical fiber sensor *Sensors Transducers J.* **125** 54–67
- [152] Elosua C, Matias I R, Barriain C and Arregui F J 2006 Volatile organic compound optical fiber sensors: a review *Sensors* **6** 1440–65
- [153] Elosua C, Matias I R, Barriain C and Arregui F J 2008 Detection of volatile organic compounds based on optical fibre using nanostructured films *Int. J. Smart Sens. Intell. Syst.* **1** 123–36
- [154] Cusano A *et al* 2009 Charge transfer effects on the sensing properties of fiber optic chemical nano-sensors based on single-walled carbon nanotubes *Carbon* **47** 782–8
- [155] Terrones S C *et al* 2006 Volatile-organic-compound optic fiber sensor using a gold-silver vapochromic complex *Opt. Eng.* **45** 44401
- [156] Elosúa C *et al* 2008 Indicator immobilization on Fabry–Perot nanocavities towards development of fiber optic sensors *Sensors Actuators B* **130** 158–63
- [157] Zhang Z H, Lockwood R, Veinot J G C and Meldrum A 2013 Detection of ethanol and water vapor with silicon quantum dots coupled to an optical fiber *Sensors Actuators B* **181** 523–8
- [158] Shobin L R, Renganathan B, Sastikumar D, Park K C and Manivannan S 2014 Pure and iso-butyl methyl ketone treated multi-walled carbon nanotubes for ethanol and methanol vapor sensing *IEEE Sens. J.* **14** 1238–43
- [159] Manivannan S, Saranya A M, Renganathan B, Sastikumar D, Gobi G and Park K C 2012 Single-walled carbon nanotubes wrapped poly-methyl methacrylate fiber optic sensor for ammonia, ethanol and methanol vapors at room temperature *Sensors Actuators B* **171–172** 634–8
- [160] Renganathan B, Sastikumar D, Srinivasan R and Ganesan A R 2014 Nanocrystalline samarium oxide coated fiber optic gas sensor *Mater. Sci. Eng. B* **186** 122–7
- [161] Kavinkumar T, Sastikumar D and Manivannan S 2015 Effect of functional groups on dielectric, optical gas sensing properties of graphene oxide and reduced graphene oxide at room temperature *RSC Adv.* **5** 10816–25
- [162] Sharifpour-Boushehri S, Hosseini-Golgoos S M and Sheikh M H 2015 A low cost and reliable fiber optic ethanol sensor based on nano-sized SnO₂ *Opt. Fiber Technol.* **24** 93–9
- [163] Ko Y, Tsai H, Lin K, Chen Y and Yang H 2017 Reusable macroporous photonic crystal-based ethanol vapor detectors by doctor blade coating *J. Colloid Interface Sci.* **487** 360–9
- [164] Konstantaki M, Klini A, Anglos D and Pissadakis S 2012 An ethanol vapor detection probe based on a ZnO nanorod coated optical fiber long period grating *Opt. Express* **20** 8472
- [165] Hromadka J, Tokay B, Korposh S, James S and Tatam R P 2015 Detection of volatile organic compounds using optical fibre long period grating modified with metal organic framework thin films *Proc. SPIE* **9634** 963435
- [166] Hromadka J, James S, Davis F, Tatam R P, Crump D and Korposh S 2015 Detection of the volatile organic compounds emitted from paints using optical fibre long period grating modified with the mesoporous nano-scale coating *Proc. SPIE* **9634** 963435
- [167] Hernandez F U, Morgan S P, Hayes-Gill B R, Harvey D, Kinneer W, Norris A, Evans D, Hardman J G and Korposh S 2016 Characterization and use of a fiber optic sensor based

- on PAH/SiO₂ film for humidity sensing in ventilator care equipment *IEEE Trans. Biomed. Eng.* **63** 1985–92
- [168] Winter G D 1962 Formation of the scab and the rate of epithelialization of superficial wounds in the skin of the young domestic pig *Nature* **193** 293–4
- [169] Williams T 2005 Humidification in intensive care *SAJC* **21** 26–31
- [170] Zuur K *et al* 2006 The physiological rationale of heat and moisture exchangers in post-laryngectomy rehabilitation: a review *Eur. Arch. Otorhinolaryngol* **263** 1–8
- [171] Santos J S *et al* 2014 Characterisation of a Nafion film by optical fibre Fabry–Perot interferometry for humidity sensing *Sensors Actuators B* **196** 99–105
- [172] Huang L *et al* 2013 Optical fibre-based sensor technology for humidity and moisture measurement: review of recent progress *Measurement* **46** 4052–74
- [173] Huang C *et al* 2015 Optical fiber humidity sensor with porous TiO₂/SiO₂/TiO₂ coatings on fiber tip *IEEE Photonics Technol. Lett.* **27** 1495–8
- [174] Corres J M *et al* 2008 Optical fiber humidity sensors using nanostructured coatings of SiO₂ nanoparticles *IEEE Sens. J.* **8** 281–5
- [175] Kang Y, Ruan H, Wang Y, Arregui F J, Matias I R and Claus R O 2016 Nanostructured optical fibre sensors for breathing airflow monitoring *Meas. Sci. Technol.* **17** 1207–10
- [176] Morisawa M, Natori Y, Taki T and Muto S 2010 Recognition of devoiced vowels using optical microphone made of multiple POF moisture sensors *Electron. Commun. Japan* **93** 12–8
- [177] Gomez D, Morgan S, Hayes-Gill B, Correia R and Korposh S 2018 Polymeric optical fibre sensor coated by SiO₂ nanoparticles for humidity sensing in the skin microenvironment *Sensors Actuators B* **254** 887–95
- [178] Akita S, Seki A and Watanabe K 2011 A monitoring of breathing using a hetero-core optical fiber sensor *Proc. SPIE* **7981** 79812W
- [179] Favero F C, Villatoro J and Pruneri V 2012 Microstructured optical fiber interferometric breathing sensor *J. Biomed. Opt.* **17** 037006
- [180] Yeo T L, Eckstein D, McKinley B, Boswell L F, Sun T and Grattan K T V 2006 Demonstration of a fibre-optic sensing technique for the measurement of moisture absorption in concrete *Smart Mater. Struct.* **15** N40–5
- [181] Hernandez F U *et al* 2017 Optical fibre sensing during critical care *Proc. SPIE* **10340** 1034012
- [182] Ledezma F U H, Correia R G, Morgan S P, Hayes-Gill B R, Evans D, Sinha R, Norris A M, Harvey D, Hardman J G and Korposh S 2016 Simultaneous temperature and humidity measurements in a mechanical ventilator using an optical fibre sensor *Proc. SPIE* **9916** 99160C
- [183] Ovington L G 2007 Advances in wound dressings *Clin. Dermatol.* **25** 33–8
- [184] Schwalfenberg G K 2012 The alkaline diet: Is there evidence that an alkaline pH diet benefits health? *J. Environ. Public Health* **2012** 727630
- [185] Waugh A and Grant A 2007 *Anatomy and Physiology in Health and Illness* 10th edn (Philadelphia, PA: Churchill Livingstone)
- [186] Pospíšilová M, Kuncová G and Trögl J 2015 Fiber-optic chemical sensors and fiber-optic bio-sensors *Sensors* **15** 25208–59
- [187] Wolthuis R, McCrae D, Saaski E, Hartl J and Mitchell G 1992 Development of a medical fiber-optic pH sensor based on optical absorption *IEEE Trans. Biomed. Eng.* **39** 531–7
- [188] Shao L-Y, Yin M-J, Tam H-Y and Albert J 2013 Fiber optic pH sensor with self-assembled polymer multilayer nanocoatings *Sensors* **13** 1425–34
- [189] Gu B, Yin M-J, Zhang A P, Qian J-W and He S 2009 Low-cost high-performance fiber-optic pH sensor based on thin-core fiber modal interferometer *Opt. Express* **17** 22296–302
- [190] Corres J M, Villar D I, Matias I R and Arregui F J 2007 Fiber-optic pH-sensors in long-period fiber gratings using electrostatic self-assembly *Opt. Lett.* **32** 29–31
- [191] Goicoechea J, Zamarreño C R, Matias I R and Arregui F J 2009 Utilization of white light interferometry in pH sensing applications by mean of the fabrication of nanostructured cavities *Sensors Actuators B* **138** 613–8
- [192] Miller W W, Yafuso M, Yan C F, Hui H K and Arick S 1987 Performance of an *in vivo*, continuous blood-gas monitor with disposable probe *Clin. Chem.* **33** 1358–65
- [193] <https://oceanoptics.com/measurementtechnique/ph-sensing/> (Accessed: 17 January 2017)
- [194] <https://presensde/products/ph/sensorshtml> (Accessed: 17 January 2017)
- [195] Tiwari G *et al* 2012 Drug delivery systems: an updated review *Int. J. Pharm. Invest.* **2** 2–11
- [196] Korposh S, Chianella I, Guerreiro A, Caygill S, Piletsky S A, James S W and Tatam R P 2014 Selective vancomycin detection using optical fibre long period gratings functionalised with molecularly imprinted polymer nanoparticles *Analyst* **139** 2229–36
- [197] Lu W X and Chen J 2003 Continuous monitoring of adriamycin *in vivo* using fiber optic-based fluorescence chemical sensor *Anal. Chem.* **75** 1458–62
- [198] Li L, Ding H, Lia B D W and Chen J 2012 Rapid detection of propofol in whole blood using an automated on-line molecularly imprinted pretreatment coupled with optical fibre detection *Analyst* **137** 5632
- [199] Barozzi M *et al* 2017 Optical fiber sensors for label-free DNA detection *J. Lightwave Technol.* **35** 3461–72
- [200] Wang X-D and Wolfbeis O S 2016 Fiber-optic chemical sensors and biosensors (2013–2015) *Anal. Chem.* **88** 203–27
- [201] Socorro A B and Díaz S 2017 Trends in fibre-optic uses for personal healthcare and clinical diagnostics ed I Matias *et al* *Fiber Optic Sensors Smart Sensors, Measurement and Instrumentation* vol 21 (Berlin: Springer)
- [202] Long F, Zhu A, Zhou X, Wang H, Zhao Z, Liu L and Shi H 2014 *Biosens. Bioelectron.* **55** 19
- [203] Singh S and Gupta B D 2013 *Sensors Actuators B* **177** 589
- [204] Coscelli E *et al* 2010 Toward a highly specific DNA biosensor: PNA modified suspended-core photonic crystal fibers *IEEE J. Sel. Top. Quantum Electron.* **16** 1–6
- [205] Queiros R B, Gouveia C, Fernandes J R A and Jorge P A S 2014 Evanescent wave DNA-aptamer biosensor based on long period gratings for the specific recognition of *E. coli* outer membrane proteins *Biosens. Bioelectron.* **62** 227
- [206] Lucas P, Solis M A, Coq D L, Juncke C, Riley M R, Collier J, Boesewetter D E, Boussard-Pledel C and Bureau B 2006 Infrared biosensors using hydrophobic chalcogenide fibers sensitized with live cells *Sensors Actuators B* **119** 355–62
- [207] Nguyen-Ngoc H and Tran-Minh C 2007 Fluorescent biosensor using whole cells in an inorganic translucent matrix *Anal. Chim. Acta* **583** 161–5
- [208] Tighe P J, Ryder R R, Todd I and Fairclough L C 2015 ELISA in the multiplex era: Potentials and pitfalls *Proteomics Clin. Appl.* **9** 406–22
- [209] Urrutia A, Bojan K, Marques L, Mullaney K, Goicoechea J, James S, Clark M, Tatam R and Korposh S 2016 Novel highly sensitive protein sensors based on tapered optical fibres modified with Au-based nanocoatings *J. Sens.* **2016** 8129387
- [210] Anderson G P, Golden J P and Ligler F S 1993 A fiber optic biosensor: combination tapered fibers designed for improved signal acquisition *Biosens. Bioelectron.* **8** 249–56

- [211] Shriver-Lake L C, Ogert R A and Ligler F S 1993 Fiber-optic evanescent-wave immunosensor for large molecules *Sensors Actuators B* **11** 239–43
- [212] Spiker J O, Kang K A, Drohan W N and Bruley D F 1998 Preliminary study of biosensor optimization for the detection of protein C *Adv. Exp. Med. Biol.* **454** 681–8
- [213] Spiker J O and Kang K A 1999 Preliminary study of real-time fiber optic based protein C biosensor *Biotechnol. Bioeng.* **66** 158–63
- [214] Moreira L *et al* 2016 Label-free optical biosensor for direct complex DNA detection using *Vitis vinifera* L *Sensors Actuators B* **234** 92–7
- [215] Chen X *et al* 2007 Real-time detection of DNA interactions with long-period fiber-grating-based biosensor *Opt. Lett.* **32** 2541–3
- [216] Sozzi M *et al* 2011 Modification of a long period grating-based fiber optic for DNA biosensing *Proc. SPIE* **7894** 78940J
- [217] Quero G *et al* 2015 Reflection-type long period grating biosensor for detection of drug resistant bacteria: the OPTObacteria project *18th AISEM Annual Conf. (Trento)* pp 1–4
- [218] Consales M *et al* 2014 Long period fiber grating biosensor for the detection of drug resistant bacteria: the ‘OPTObacteria’ project *3rd Mediterranean Photonics Conf. (Trani)* pp 1–3
- [219] Chiavaioli F *et al* 2015 Sol-gel-based titania–silica thin film overlay for long period fiber grating-based biosensors *Anal. Chem.* **87** 12024–31
- [220] Biswas P *et al* 2017 Design, fabrication and characterisation of silica-titania thin film coated over coupled long period fibre gratings: towards bio-sensing applications *Sensors Actuators B* **253** 418–27
- [221] Caucheteur C, Guo T and Albert J 2015 Review of plasmonic fiber optic biochemical sensors: improving the limit of detection *Anal. Bioanal. Chem.* **407** 3883
- [222] Guo T *et al* 2017 Plasmonic optical fiber-grating immunosensing: a review *Sensors* **17** 2732
- [223] Albert J, Lepinay S, Caucheteur C and DeRosa M C 2013 High resolution grating-assisted surface plasmon resonance fiber optic aptasensor *Methods* **63** 239–54
- [224] Singh S and Gupta B D 2013 Fabrication and characterization of a surface plasmon resonance based fiber optic sensor using gel entrapment technique for the detection of low glucose concentration *Sensors Actuators B* **177** 589–95
- [225] Silvestri S and Schena E 2011 Optical-fiber measurement systems for medical applications *Optoelectronics—Devices and Applications* ed P Predeep (Rijeka: InTech) (<https://doi.org/10.5772/18845>)
- [226] Dymond *et al* 2012 Developing a new treatment device: how to get an idea to the marketplace *Neurorol. Urodyn.* **31** 429–36
- [227] Gold H T, Pitrelli K, Hayes M K and Murphy M M 2014 Decision to adopt medical technology: case study of breast cancer radiotherapy techniques *Med. Decis. Mak.* **34** 1006–15
- [228] Piau A, Campo E, Vellas B and Nourhashemi F 2016 Development of new technologies for healthy aging: searching for the right way *J. Aging Res. Clin. Pract.* **5** 61–4
- [229] Rogers E 2003 *Diffusion of Innovations* 5th edn (New York: Free Press)
- [230] WHO 2010 Barriers to Innovation in the Field of Medical Devices: Background Paper 06, August <http://apps.who.int/medicinedocs/en/d/Js17701en/> (Accessed: 14 January 2018)
- [231] Campbell B, Dobson L, Higgins J, Dillon B, Marlow M and Pomfret C A 2017 New health technology assessment system for devices: the first five years *Int. J. Technol. Assess. Health Care* **33** 19–24
- [232] Campbell B 2013 Regulation and safe adoption of new medical devices and procedures *Br. Med. Bull.* **107** 5–18
- [233] Jzerman M J I, Koffijberg H, Fenwick E and Krahn M 2017 Emerging use of early health technology assessment in medical product development: a scoping review of the literature *PharmacoEconomics* **3** 727–40
- [234] Cosh E, Girling A, Lilford R, McAteer H and Young T 2007 Investing in new medical technologies: a decision framework *J. Commer. Biotechnol.* **13** 263–71
- [235] Lu B, Martin J L, Craven M P and Morgan S P 2012 Can health economics aid decision making in healthcare innovation in academia? *Int. J. Technol. Transfer Commercialisation* **11** 70–87
- [236] Vincent C J, Li Y and Blandford A 2014 Integration of human factors and ergonomics during medical device design and development: it’s all about communication *Appl. Ergon.* **45** 413–9
- [237] Martin J L, Norris B J, Murphy E and Crowe J A 2008 Medical device development: the challenge for ergonomics *Appl. Ergon.* **39** 271–83
- [238] Zhang L, Li Z, Mu J, Fang W and Tong L 2015 Femtoliter-scale optical nanofiber sensors *Opt. Express* **23** 28408–15